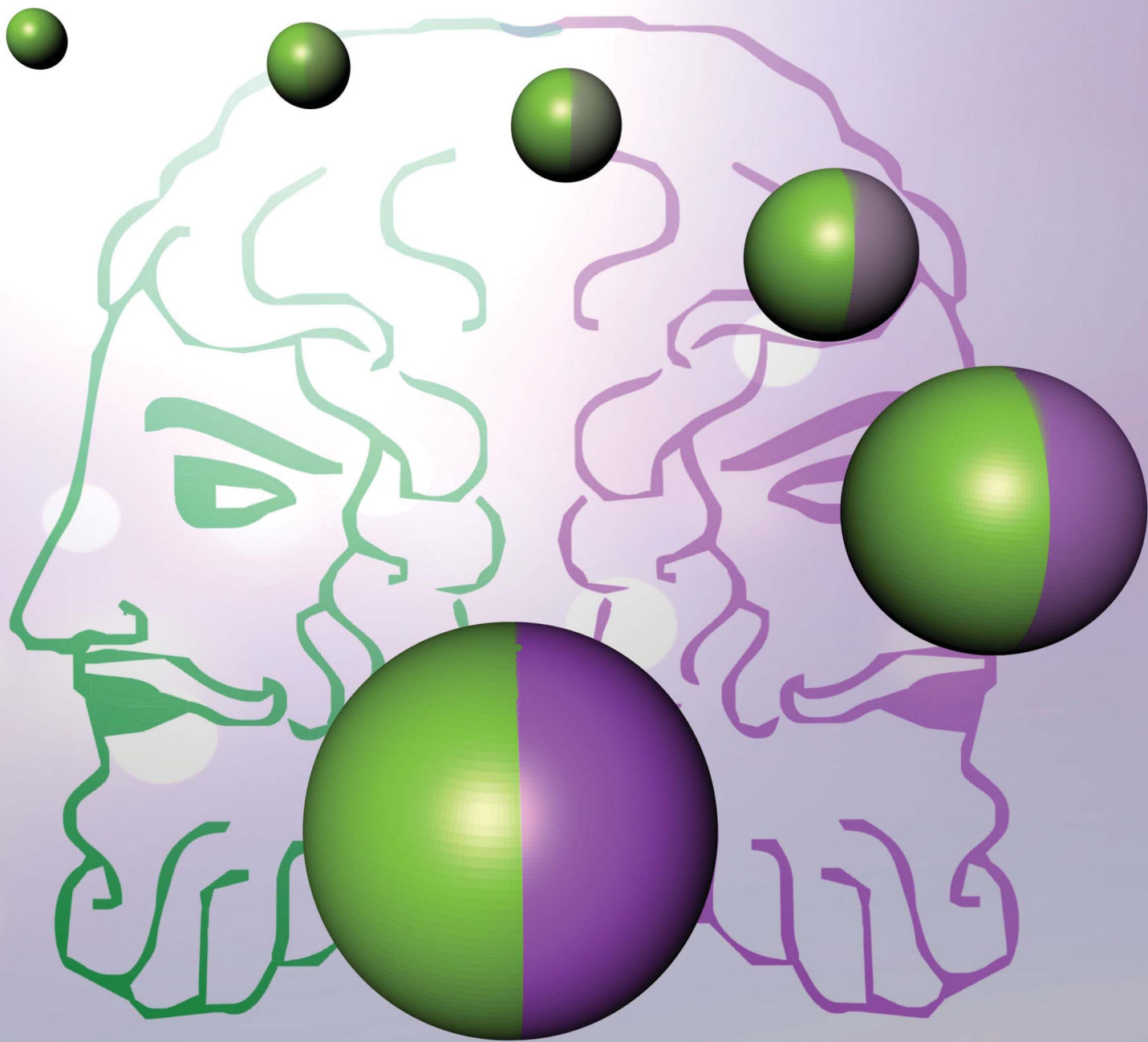


Journal of Materials Chemistry

www.rsc.org/materials

Volume 22 | Number 31 | 21 August 2012 | Pages 15429–16146



ISSN 0959-9428

RSC Publishing

FEATURE ARTICLE

Gabriel Loget and Alexander Kuhn

Bulk synthesis of Janus objects and asymmetric patchy particles



0959-9428 (2012) 22:31;1-F

Bulk synthesis of Janus objects and asymmetric patchy particles

Gabriel Loget and Alexander Kuhn*

Received 20th March 2012, Accepted 10th May 2012

DOI: 10.1039/c2jm31740k

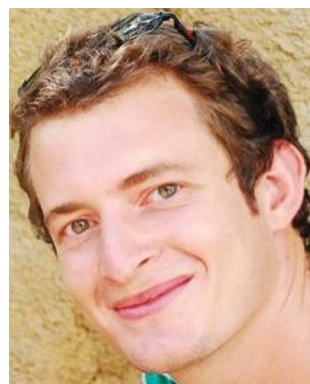
This review article highlights the most recent advances with respect to the preparation of Janus objects by bulk phase processes. Historically most of the concepts developed for generating asymmetric particles have been based on the use of interfaces or surfaces, which are necessary to break the symmetry. This restricts in many cases the amount of produced particles, due to the two-dimensional nature of the approaches. Therefore the bulk synthesis of such asymmetric micro- and nanoobjects is of primary importance for their production at an industrial scale and helps to open up the field to commercial applications. We summarize here the different alternative concepts, spanning a wide range from sophisticated polymer chemistry to the use of external electromagnetic fields, that have been proposed in recent years in order to break the symmetry in true bulk processes.

1. Introduction

Janus was one of the major roman gods and was usually represented with two faces looking in opposite directions (Fig. 1a). Being the god of time, beginnings, endings and transitions, he was also the god of gates and doors, hence we can still find his presence in the word “janitor” (gatekeeper). In reference to the god’s facial features, De Gennes coined in the late eighties the term “Janus grains”.^{1,2} He used it for describing particles that,

similar to amphiphilic molecules, were composed of two different parts, one being hydrophilic and the other being hydrophobic. After De Gennes’ introduction, the term “Janus particle” was usually employed for describing objects with sizes ranging from the micro- to the nanoscale owing to different chemistries or polarities and thus, structures exhibiting a chemical break of symmetry.^{3,4} Asymmetry at the nanoscale can be found in nature, a good example being hydrophins. These proteins that are produced by filamentous fungi show a hydrophobic patch composed of chain residues of leucine, valine and alanine which occupy 20% of their surface.⁵ From this chemical asymmetry very interesting properties are arising, such as a surfactant

Université de Bordeaux, ISM, UMR 5255, ENSCBP, 16 avenue PeyBerland, 33607 Pessac, France. E-mail: kuhn@enscbp.fr; Fax: +33 5 40 00 27 17; Tel: +33 5 40 00 65 73



Gabriel Loget

Gabriel Loget received his bachelor degree in Chemistry and master degree in Molecular Chemistry from University of Rennes (France). He is currently working on his PhD at the University of Bordeaux (France) under the supervision of Pr. Alexander Kuhn. His research mainly focusses on developing new concepts for synthesis of Janus-type objects and locomotion of particles.



Alexander Kuhn

Alexander Kuhn obtained a master degree in Chemistry from the Technical University of Munich (Germany) and a PhD in Physical Chemistry from the University of Bordeaux (France). After a post-doc position at the California Institute of Technology (USA) he moved to the University of Bordeaux as an assistant professor and is since 2000 a full professor. His main research interests are in electrochemistry, surface modification and nano-science. In recent years he has

made contributions to the fields of bioelectrochemistry, electro-analysis, the rational design of electrode surfaces and the synthesis of micro- and nanoobjects that can be used, among others, as autonomous swimmers.

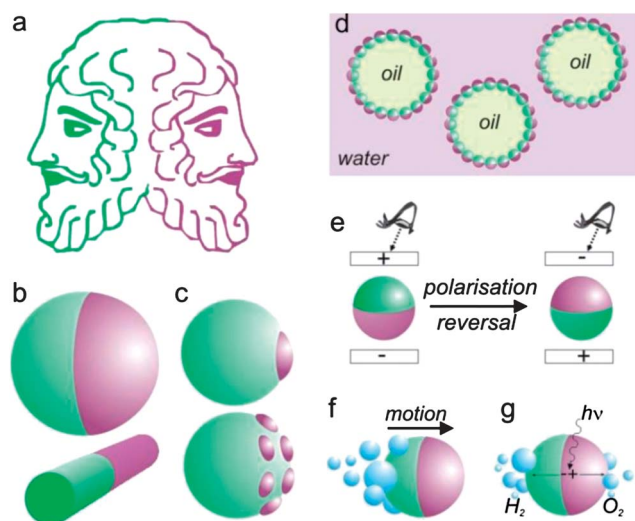


Fig. 1 (a) Two-faced god Janus. (b) Janus particles (JPs), isotropic (top) and anisotropic (bottom). (c) Asymmetric patchy particles (APPs). (d) JPs as emulsion stabilizers. (e) Electrophoretic rotation of a JP between two transparent electrodes. (f) Janus swimmer propelled by bubble generation at one side of the object. (g) Electron-hole photogeneration at a metal-semiconductor Janus interface for water splitting.

behavior with self-assembly at water-air interfaces⁶ which are already exploited for stabilizing emulsions.⁷ In the last few years the term Janus has been increasingly employed beyond the frontiers of micro- and nanochemistry. One can find in the recent literature for example publications dealing with “Janus macromolecules” such as dendrimers⁸ and fullerenes.⁹ As the following review is focused on asymmetric particles at the micro- and nanoscale, this topic will not be developed.

A very wide range of particles with different chemistries and shapes is now available and their complexity is increasing due to the variety of techniques that emerge as nanotechnology is developing. It therefore becomes necessary to establish a precise classification that is likely to be accepted by the scientific community.¹⁰ In this context, even if the term “Janus particle” was widely used, Du and O'Reilly recently clarified the description of asymmetric particles.¹¹ Based on their definitions, we will distinguish between “Janus” and “patchy” particles.

The term “Janus particles” (JPs) will be employed when the object is composed of equally separated domains (Fig. 1b) in contrast to “asymmetric patchy particles” (APPs) for systems with non-equally separated domains (Fig. 1c). The generic term “asymmetric particles” (APs) will be used when describing both of them. Although increasing efforts are made to create different sorts of patchy particles (PPs),^{11–13} symmetrical patchy particles will not be discussed, as the main focus of the present review is the physico-chemical asymmetry of the particles.

JPs and APPs can be isotropic or anisotropic (Fig. 1b), they can have plenty of different shapes and can be constituted of many materials, which can be either hard or soft. A straightforward approach for producing APs, introduced by Casagrande in 1988,¹ that is still used in many laboratories consists of immobilizing particles at an interface for breaking the symmetry. Even if these interface-based techniques allow a very good regularity in functionalisation, they make the preparation of

large quantities rather difficult, because they usually lead to monolayer equivalents of material as the modification occurs in a two-dimensional reaction space. In his 1992 Nobel Prize lecture, De Gennes already mentioned the importance of scaling-up the production of dissymmetric objects.² Obviously, for their commercialization and their use at an “industrial scale”, bulk techniques for producing APs need to be developed. Consequently, in the recent literature, one can notice intensive efforts made in this direction. Even if several articles^{10,14,15} and excellent reviews, discussing the synthesis of JPs and PP, already exist,^{4,3,11,16–24} none of them focuses on the bulk synthesis. Therefore, it seems timely to discuss techniques that have a potential chance to be used for an up-scale of AP production. In this review, the utility of APs will be discussed, then, one and two dimensional synthetic techniques will be briefly presented, and finally the bulk techniques for breaking the symmetry will be reviewed.

2. Behavior of Janus and asymmetric patchy particles

2.1. Adsorption at interfaces and self-assembly

Because of their intrinsic heterogeneities, one of the first properties of Janus and asymmetric patchy particles that naturally comes into one's mind is their assembly at interfaces, and intensive work has been carried out to observe and understand this phenomenon. De Gennes illustrated the assembly of JPs at interfaces using the expression: “*The skin can breathe*”, imagining a monolayer of “*Janus grains*” like a membrane with “*pores*” between the grains, allowing the exchanges between the two separated media.² Organization of poly(methyl methacrylate) (PMMA) and polystyrene (PS) JPs at the water-air interface has been observed by Xu *et al.*²⁵ and several theoretical studies have been performed to predict JP behavior at liquid-liquid interfaces. Binks *et al.* performed calculations in order to compare the adsorption of homogeneous spherical silica particles to asymmetric ones at the oil-water interface. It was found that by maximizing the amphiphilicity of particles, desorption energies can be increased by a factor of three.²⁶ Nonomura *et al.* estimated the adsorption energy for $\sim 10 \mu\text{m}$ diameter Janus disks at a liquid-liquid interface as about 10^8 to $10^9 k_B T$.²⁷ Considering these data and combining them with the Pickering effect, the strong potential for APs to be used as particulate surfactants becomes obvious (Fig. 1d). Comparable to the hydrophilic-lipophilic balance (HLB) for amphiphilic molecules, the notion of “Janus balance” was introduced by Jiang and Granick as the ratio of work to transfer a JP from the oil-water interface into the oil phase and the work needed to move it into the water phase.²⁸ This value (that can also be applied to homogeneous particles) is calculated with simple parameters and gives information about the particle adsorption and can help in designing efficient asymmetric particle emulsifiers. Hirose studied theoretically the adsorption of spherical submicron APs at curved interfaces, and concluded that liquid droplets surrounded by Janus particles may be stable and can be considered as a soft solid.²⁹ Ruhland *et al.* measured interfacial tensions at liquid-liquid interfaces using submicrometer and micrometer-sized PMMA-PS Janus disk stabilizers.³⁰ A very nice practical study

of micrometer-sized spherical JPs at the oil–water interface was carried out by Park *et al.*³¹ It has been shown that, in contrast to homogeneous particles, JPs were attracted to each other due to capillary interactions generated by the irregular shape of the Janus boundary. A control of the inter-particle interactions offset based on electrostatic repulsions was also demonstrated.³¹ Adams *et al.* also insisted on the importance of the Janus boundary quality and its roughness for the adsorption at air–water and water–oil interfaces.³² Considering nanometer-sized JPs, based on data obtained by Monte-Carlo simulations, Cheung and Bon emphasize the fact that at these scales, the particles are more affected by Brownian motion, and one has to carefully consider their orientational freedom.³³ Glaser *et al.* measured a considerable decrease of the interfacial water–hexane tension using ~ 10 nm APPs compared to homogeneous particles of comparable size and chemical nature.³⁴

2.1.1. Particulate surfactants. Several groups used Janus and APPs as particulate surfactants. Polymeric and silica micrometer and submicrometer-sized APPs with different morphologies were used for stabilizing emulsions (Fig. 1d).^{35,36} Recently, more complex and very interesting systems were developed. Firstly, Tanaka *et al.* showed the control of the Janus balance on mushroom-like asymmetric particles upon stimuli such as temperature and pH, resulting in stabilization/destabilization of emulsions under different conditions.³⁷ Secondly, Liang *et al.* used tailored Janus nanosheets as particulate surfactants. Modification of one side of the sheets with paramagnetic particles allowed manipulation of the droplets with a magnetic field.³⁸ Particulate surfactants owning catalytic parts make them very attractive catalysts for reactions where reactants and products are soluble in different phases.³⁹ Such a system was elegantly presented by Crossley *et al.* for improving biofuel upgrade reactions.⁴⁰

2.1.2. Stabilizers in polymer systems. Advanced materials can be obtained by blending non-miscible polymers. In order to be successful, the blending requires the use of compatibilizing agents, often block copolymers, which generates several problems such as micellisation and non-specific adsorption of the agent.⁴¹ In order to overcome the problems, Walther *et al.* demonstrated the use of JPs as very efficient stabilizers for PMMA and PS blends.⁴¹ Simulations were also recently performed in order to predict the incorporation of JPs into macroscopically oriented structures of diblock copolymers.⁴² Interestingly, it was recently observed that JPs can be spontaneously generated in quaternary polymer blends.⁴³

In a similar way Janus particles have been used for emulsion polymerization of PS, styrene and *n*-butylacrylate without additives.⁴¹ The sizes of the monodisperse PS latexes that can be obtained are controlled by the amount of added Janus particles.⁴¹

2.1.3. Water repellents. Morphologies and wetting properties of silica wafers coated with micrometer-sized spherical asymmetric polymeric particles (hydrophilic/hydrophobic) were recently studied and compared to homogeneous particles.⁴⁴ Surfaces coated with homogeneous particles showed a hydrophobic behavior, while, due to APs self-assembly into aggregates, surfaces coated with them were super-hydrophobic.⁴⁴ Kim *et al.*

prepared microstructured JPs that were used for conceiving flexible hydrophobic surfaces and liquid marble that can be manipulated with tweezers.⁴⁵ The possibility to use JPs to make water repellent textiles has also been demonstrated recently.⁴⁶

2.1.4. Asymmetric particles as membrane key-components. Based on computer simulations, Alexeev *et al.* predicted that combining a lipid membrane and APs could lead to a new kind of membrane.⁴⁷ When the membrane is stretched, pores can open that close again when the tension is released. In the presence of APs, which will be located at the inner pore wall, the pore is stabilized allowing for an “open door” for exchanges through the membrane.⁴⁷

2.1.5. Self-assembly of asymmetric particles. APs, like amphiphilic molecules, have the ability to self-assemble into superstructures. This phenomenon is very interesting from an intellectual as well as from a practical point of view and could be used to mimic molecular behaviour.^{10,21} Experimentally, Park *et al.* showed that micrometer-long gold/polypyrrole nanorods arrange themselves in solution, giving rise to fascinating structures (from bundles to core–shell hollow spheres) that can be controlled by tailoring the rod morphology.⁴⁸ Walther *et al.* studied the assembly of PMMA–PS Janus cylinders, showing that above a certain critical concentration or in certain solvents fiber-like superstructures constituted of cylinders with a PS domain at the centre are formed.⁴⁹ Theoretically, first simulations of the patterns that can be formed by JPs self-assembly were performed in a very simplified 2D model.⁵⁰ Granick’s team carried out very important work based on simulations and experimental observations to further understand JPs assembly.²² Simulations and experiments revealed that dipolar spherical JPs will form clusters with a preserved charge anisotropy (in the case where the particle diameter is higher than the electrostatic screening length).⁵¹ A second approach, based on experiments and a model considering charged/hydrophobic spherical JPs also predicted the formation of small clusters.⁵² A very interesting element revealed in this case is that the size of the cluster can be controlled by the salt concentration. At low ionic strength, the electrostatic repulsion between JPs will dominate the hydrophobic interactions, leading to small clusters. Increasing the salt concentration will lead to bigger clusters with very interesting morphologies such as worm-like structures or a chiral triple helix.^{52,53}

2.2. Dynamics in magnetic and electromagnetic fields

2.2.1. Orientation control of Janus particles in electric DC and magnetic fields – towards pixels for e-paper. Electronic paper (e-paper) is a display technology designed to imitate the paper appearance for objects such as mobile phones and e-book readers. The majority of e-paper technologies are based on electrophoretic screens, the display being constituted of vesicles, acting as pixels, which are filled with black and white particles owning opposite charges. With each vesicle being sandwiched between transparent electrodes, switching their polarity results in attracting particles with different charges and colours towards the reader’s eye.⁵⁴ One can easily imagine that JPs are very suitable objects to increase the performance of such

a technology. This would avoid the use of vesicles and allow for increasing the display resolution since in this case each JP can act as a pixel (Fig. 1e). Indeed, dipolar JPs will orientate in DC electric fields as it has been demonstrated with gold–latex JPs⁵⁵ and with gyricon balls.⁵⁶ This phenomenon has already been used for conceiving electrophoretic screens with electrically anisotropic 100 μm black/white⁵⁷ and 300 μm black/green⁵⁸ Janus beads. Very recently, a magneto-driven display has been introduced with Janus beads containing Fe_3O_4 nanoparticles (NPs) at one side and fluorescent quantum dots at the other side.⁵⁹

2.2.2. Motion and assembly in AC electric fields and magnetic fields. Velev's group carried out pioneering work by studying experimentally the behaviour of JPs in external fields.⁶⁰ As it has been predicted by Bazant and Squires,^{61,62} APs composed of materials with different polarisability move in homogeneous AC electric fields (ACEFs).⁶³ Micrometer-sized PS–gold JPs have been studied in low-frequency ACEFs. First, due to the largest induced dipole orientation in the field direction, they orientate with the boundary being parallel with respect to the ACEF direction. Then, submitted to induced charge electrophoresis,^{61,62} they move normally to the electric field towards the PS part (Fig. 2a).⁶³ In fact, the induced double layer of the metal part being composed of much more counter-ions than at the insulating part, the ions will move tangentially to the electric field direction, dragging liquid and thus generating the motion

(Fig. 2a, inset).⁶³ Due to the electric field induced dipole interactions between the same JPs, at higher frequencies ACEFs, they assemble in staggered chains, 3D bundles or 2D crystals (Fig. 2b and c) and disassemble when the field is switched off.⁶⁴ Micrometer-sized PS–iron JPs, can assemble in ACEFs as well as in magnetic fields.⁶⁵ Depending on the coating thickness, different JP chain morphologies can be formed, which persist when the magnetic field is removed and can be disassembled by demagnetisation.⁶⁵ APs containing a p-type material–metal junction exhibit a diode-like behaviour.⁶⁶ Chang *et al.* have shown that diodes can be moved in a controlled way in ACEFs.⁶⁷ Indeed, the diode rectifying effect generates an electroosmotic flow at its proximity which directs the motion.⁶⁷ Recently, Calvo-Marzal *et al.* propelled cadmium–polypyrrole APs in ACEFs at a micrometer-scale.⁶⁸

2.2.3. Manipulation with optical and optomagnetic traps and motion in a laser beam. In contrast to dielectric micro/nanoparticles and metallic NPs that can be manipulated in three dimensions in optical traps, metallic microparticles and micro-JPs with a metal part can only be controlled in two dimensions due to inhibited light transmission by the metal coating.⁶⁹ This lowers their spatial control in optical traps, but can also provide an original way to generate a JP rotational motion above a certain laser power.⁷⁰ Erb *et al.* showed for the first time that micrometer-sized spherical APPs with a metallic patch can be controlled in three dimensions by optical tweezers.⁶⁹ Using a cobalt patch, they were able to control two additional degrees of freedom in an optomagnetic trap.⁶⁹ Besides the optical tweezer context, Jiang *et al.* used a defocused laser beam to propel silica–gold micrometer-sized Janus beads by self-thermolysis, the motion being directed by the temperature gradient generated by the laser light absorption in the gold part.⁷¹

2.3. Chemically and magnetically driven micro- and nanoswimmers

Autonomous microswimmers are of enormous interest for practical applications such as drug delivery,⁷² DNA detection,⁷³ isolation of cancer cells⁷⁴ and writing of microstructures.⁷⁵ The swimmers are APPs with catalyst patches that can be used to generate a linear motion. Several strategies have been developed and the motion can be generated using magnetically and/or chemically active patches containing a ferromagnetic material,^{76–79} enzymes⁸⁰ or enzyme mimics.⁸¹ The most developed strategy consists of using the hydrogen peroxide decomposition reaction at a metal catalyst patch for generating the motion by self-electrophoresis⁸² or a bubble propulsion mechanism.^{83,84} (Fig. 1f). This research area becomes very attractive and a lot of efforts are made by different groups, and one can cite as examples work carried out by Wang *et al.*,^{85–88} Mallouk *et al.*,^{89,90} Sen *et al.*^{91,92} and Ozin *et al.*^{93,94} For more information, we refer the interested reader to recent reviews and perspective articles.^{95–100}

2.4. Asymmetric particles for sensing

As was discussed previously, APs orientate in a DC electric field. As this orientation ability depends on the surface charges, one

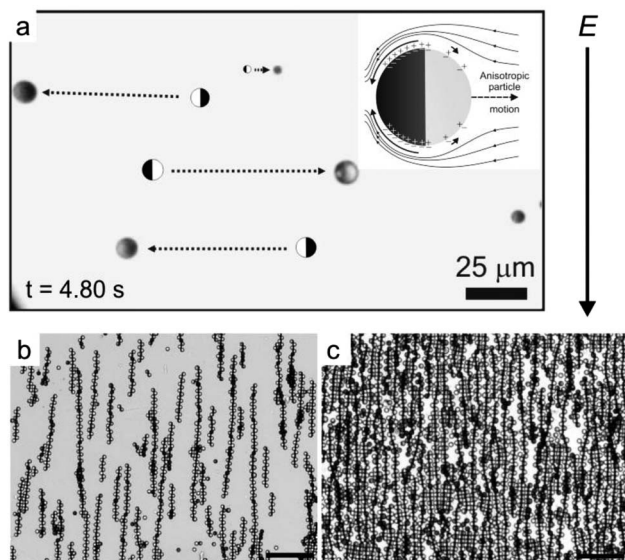


Fig. 2 (a) Optical images illustrating motion of PS–gold JPs in an AC field of amplitude 140 V cm^{-1} and 1 kHz frequency, JP positions at $t = 0$ s are represented by drawings. Inset: scheme of induced charge electrophoresis responsible for the motion. Reprinted with permission from ref. 63 Copyright (2008) by The American Physical Society. (b) Optical micrograph of staggered chains of PS–gold JPs formed at 56 V cm^{-1} at 40 kHz; the scale bar represents 70 μm . Reprinted with permission from ref. 64 Copyright (2008) American Chemical Society. (c) Optical micrograph of a metallo-dielectric 2D lattice of confined staggered chains formed at 27 V cm^{-1} at 40 kHz with a higher JP concentration; the scale bar represents 50 μm . Reprinted with permission from ref. 64 Copyright (2008) American Chemical Society. The field direction for the three figures is indicated by the upright arrow.

can use APs functionalized on one part with a pH dependent charged molecule to make a pH sensor.⁵⁵ 5 nm magnetic APPs owning pH or temperature sensitive polymer patches have been synthesized. Since these parameters affect the agglomeration state of the PPs by hydrophobic forces and electrostatic repulsions, their precipitation can be considered as a sensor output signal.¹⁰¹ Himmelhaus and Takei conceived an optical detector with arrays of ~ 100 nm spherical PS–gold JPs having a homogeneous alignment (the PS half facing the substrate).¹⁰² Because the maximum wavelength of the array's extinction peak depends on the refractive index of the media and on the compounds binding to the gold half spheres, these systems can be used for *in situ* sensing of self-assembled monolayer formation and binding of biomolecules.¹⁰² Microsized JPs with fluorescent metal half spheres in suspension show fluorescent patterns, which look like the moon phases, from which information about the four degrees of freedom can be deduced.¹⁰³ Magnetic fluorescent metal JPs (MagMOONs) rotating with an external magnetic field, can be very useful for detection in biological environments, since the periodic blinking of the JPs allows an easy *in situ* background subtraction.^{104–108} The free motion of similar systems in solution due to Brownian motion can be used for conceiving modulated optical nanoprobes (MOONs). The autocorrelation function of the fluorescence fluctuation of the blinking MOONs allows precise detection of parameters such as temperature, pressure, viscosity, chemical interactions and influences of the environment.^{109–111}

2.5. Interaction with light: plasmon materials, anti reflecting-surfaces and photocatalytic applications

Wang and Halas studied experimentally plasmonic properties of arrays made of ~ 200 nm dumbbell-like gold nanoshell APs.¹¹² The polyvinylpyridine coated parts of the AP are embedded into PDMS, so that each AP side faces different dielectric environments, leading to non-similar plasmon modes that hybridize.¹¹² In another context, it was reported that PS snowman-like AP arrays on glass show a transmittance increase compared to glass with a single layer of spherical PS particles. This so-called mothe effect can be very useful for designing anti-reflective coatings.¹¹³ Photogeneration of electron–hole pairs upon photoexcitation of semiconducting (SC) material can be used for applications such as depollution, synthesis and water splitting. However, photocatalytic activity of sole SC particles is usually poor and leads to high charge recombination rates. Adding a metallic junction to the SC particles is a strategy that can be used to increase the photocatalytic yields. Indeed, the metal part acts as an “electron sink”, due to its larger electric double layer capacitance compared to the SC one, and therefore a SC–metal junction decreases the charge recombination probability.¹¹⁴ Gold–TiO₂ snowman-shaped APs with sizes around 10 nm have been studied for photocatalytic applications. This system showed an increased activity for methanol oxidation compared to TiO₂ NPs.¹¹⁴ AP arrays were also more active for methylene blue degradation compared to TiO₂ and gold–TiO₂ composite NPs.¹¹⁵ These results suggest that SC–metal APs can be used as efficient photocatalysts, and one can imagine that photon-induced water splitting may be achieved in the near future by engineering the JPs components (Fig. 1g).

2.6. Medical applications

Even if so far no *in vivo* medical application has been developed, it is straightforward to imagine the strong potential of APs for *in vivo* drug delivery since one part of the particle can play the role of the recognition unit (for disease affected body area recognition), with the other part being the drug carrier. Hu and Gao recently reported imaging and magnetolytic therapy based on the use of JPs.¹¹⁶ 100 nm fluorescent magnetic APPs have been magnetically directed for staining cells. Once the cells are stained, they can be imaged and destroyed under the action of a rotating magnetic field.¹¹⁶

3. Breaking the symmetry at a single interface, one and two-dimensional synthetic approaches

We will now briefly discuss some classic approaches that have been used for APs synthesis at single interfaces. They are based on solid–liquid, liquid–liquid, liquid–gas and gas–solid interfaces, and as a consequence, the synthesis is carried out in a one or two dimensional reaction space. Multistep procedures are required for two-dimensional approaches and they are strongly limited by low space-time yields. However, they usually lead to APs with a good homogeneity, and sufficient quantities for laboratory use, but up-scaling of these processes to an industrial level is more difficult to imagine.

3.1. Interface immobilization and modification

A straightforward, first published¹ and probably most used technique to break symmetry consists of modifying objects that are immobilized at an interface, so that a part of the objects is screened and cannot be modified. Even if the panel of accessible APs using this approach is very large and the quality of the obtained APs is rather good, the synthesis is quite tedious since multiple steps are required (Fig. 3a). Particle immobilization in a compact array can be achieved by techniques such as Langmuir–Blodgett,^{117,118} spin coating,¹¹⁹ drop casting,¹²⁰ solvent evaporation,^{121,122} convective assembly,^{123,124} and spreading on

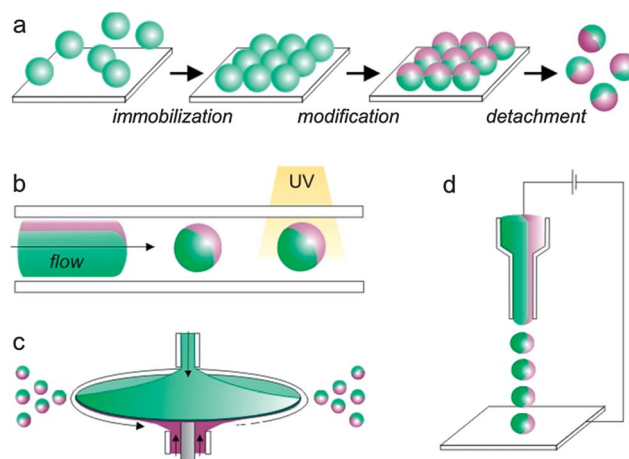


Fig. 3 (a) Janus particle synthesis by modification of immobilized spherical particles. (b) Formation of Janus particles based on microfluidics. (c) Gyration process. (d) Janus particle formation by the electrodynamic co-jetting process.

a liquid–air¹²⁵ or a liquid–liquid¹²⁶ interface. Subsequently, a polymer can be added to protect the particle's lower surface for a precise boundary adjustment.^{1,119,124,127,128} The surface modification can be achieved by a wide range of techniques among which one can cite molecular functionalisation,^{119,129} electrostatic adsorption,^{125,130} microcontact printing using a polydimethylsiloxane (PDMS) stamp,^{112,113,121,131} metal sputtering,^{120,132} temperature change,¹²⁶ plasma polymerization,^{127,133} electroless deposition,¹²⁴ electrophoretic modification,¹²² electrochemical deposition¹²⁸ and Langmuir–Blodgett film transfer.¹³⁴ Finally, after having removed the protecting polymer by dissolution, the particle can be detached, usually by sonication.

3.2. Template-based synthesis

Templates are interesting supports for breaking symmetry. A recent approach is based on the use of colloidal crystals. After a surface functionalisation of the colloidal crystal, the removal of the first bead layer is achieved with tape, revealing the beads underneath with unfunctionalized surface dots at their top. These “naked” silica dots can be used as active surfaces to grow patches asymmetrically.¹³⁵ Yin *et al.* studied geometric confinement induced by dewetting along surfaces patterned with holes.¹³⁶ They elegantly showed that PS and silica particles can be confined in cylindrical holes with appropriate diameters. Heating the template filled with the beads above the PS glass transition temperature allows welding of the particles, leading to micrometer-sized APPs.¹³⁷ Electrodeposition through porous membranes such as alumina or track etched polycarbonate is a common technique for producing metallic or semiconducting nanotubes.¹³⁸ This multi-step technique which requires (i) evaporation of a metallic layer on one side of the film to serve as a working electrode, (ii) electrodeposition and (iii) membrane dissolution, can be used to create multi-component asymmetric tubes.^{48,93,138,139}

3.3. Self-assembly by colloidal crystallization and coalescence

Velev *et al.* showed that water evaporation from droplets containing latex beads, previously spread at a perfluorinated liquid–air interface can result in microstructured particles.¹⁴⁰ Segregation of different colloids in the droplets can lead to AP generation.¹⁴⁰ A dielectrophoresis chip was elaborated so that evaporating droplets can be moved during the crystallization process.¹⁴¹ Fialkowski *et al.* developed an original method based on the use of a glass surface covered with a water soluble gel substrate.¹⁴² After hydrophobic droplets, containing different pre-polymers, are deposited on the gel layer, they can coalesce to form one dissymmetric droplet at the gel–air interface. The gel is then etched which, by decreasing the gel–droplet contact area, can induce the generation of a spherical Janus droplet that can be solidified by heating or UV exposure.¹⁴² A similar concept was developed on a dielectrophoresis-chip where the coalescence of water droplets with different compositions on a perfluorinated liquid–air interface can be controlled by using electric fields.¹⁴³

3.4. Microfluidic approaches

Microfluidic devices are getting more and more popular for the production of a large range of particles, among which one can

find APs and especially JPs.¹⁴⁴ A three-channel hydrodynamic device with an inner gas channel located between two outer channels containing liquids with different particles can be used to create Janus shells by the assembly of the particles around the gas bubble.¹⁴⁵ A Y-shaped channel can be used to form a two phase organic stream containing monomers and colloids. Upon encountering in a co-flowing aqueous stream, the organic one can form Janus droplets with colloidal,⁵⁷ color^{57,58,146} or molecular anisotropy.¹⁴⁷ The droplets are finally solidified by heat treatment⁵⁷ or UV-curing (Fig. 3b).¹⁴⁷ It is noteworthy that Nisisako and Torii developed a chip with 128 outlet channels for the laboratory-scale production of JPs.¹⁴⁸

3.5. Electrodynamic co-jetting

Electrospinning is a common technique for producing polymer fibers. Basically, a high electric field applied between the solution and a counter-electrode located underneath induces a jet of electrically charged species directed towards the substrate, which after solvent evaporation and solidification will usually lead to fibers. Lahann's group, using an electrospinning setup, showed that the effect of a high electric field on a laminar flow of two polymers can eventually lead to the generation of micrometer and sub-micrometer APs (Fig. 3d).^{149,150} Naturally, Janus fibers can also be obtained.¹⁵¹

4. One and two dimensional approaches with high production rates

Even if they usually lead to high-quality and uniform APs, it seems obvious that the great majority of the one or two-dimensional techniques presented above can hardly be considered for industrial production of APs, since they are limited by low space-time yields due to the use of individual interfaces. A couple of low-dimensional methods, which we will present below, seem to be quite attractive, since they show that in some cases, inherent disadvantages can be balanced, thus leading to higher production rates.

4.1. Spinning disk process

“Gyricon” beads are bicolored micrometer-sized JPs produced by Xerox for applications in e-paper.^{56,152} Their synthesis is based on the spinning disk process (Fig. 3c).¹⁵³ Basically, two differently pigmented molten polyethylene streams are projected respectively onto both sides of a spinning disk (~3000 rpm). The centrifugal force makes these streams flow to the disk edge where they encounter. Here, affected by the Taylor instability, the stream is ejected as small jets formed by bicolored JP spheres, with a size from 40 to 106 μm, depending on the disk rotation rate, and which then solidify as they fly away from the disk.¹⁵³

4.2. Breaking the symmetry in electrospun fibers

Ho *et al.* reported a technique for generating APs based on the immobilization of silica particles at the surface of large surface area electrospun fibers.¹⁵⁴ The particle embedding can be triggered by the spinning temperature, leading to a control over the APs boundaries (Janus balance). After a surface treatment on the uncovered part, anisotropically modified particles can be

released from the fibers by a simple washing process. The technique has been validated by the synthesis of 500 nm sized Janus beads with one half covered with gold NPs. The authors achieved the production of billions of APs per mg of polymer mat.¹⁵⁴

5. Breaking the symmetry at interfaces in the bulk

An obvious strategy that one can consider for increasing the yield of AP formation consists of developing similar techniques than the ones previously described at interfaces, but trying to increase the size of the interface as much as possible. Accessible interface areas increase exponentially when using emulsions and suspensions, an aspect that has already been considered for creating APs.

5.1. Pickering emulsions

In order to decrease the surface energies of emulsion interfaces, particles tend to adsorb strongly at these interfaces to stabilize the emulsion. This so-called Pickering effect has been used to produce APs in large quantities.

5.1.1. Liquid–liquid Pickering emulsions. When the particles are adsorbed at the Pickering interface, one part is immersed in the oil phase, while the other one is immersed in the water phase, which allows topo-selective modifications. Usually, a tuning of the functionalised areas is possible, since the particle embedding in the droplet depends on the droplet polarity and on the particle's surface hydrophobicity. Using the adsorption of spherical metal NPs at oil–water emulsion interfaces, combined with the reduction of silver, allowed the synthesis of bimetallic nanometer-sized APPs.¹⁵⁵ Modification of the water accessible surface of CuO microbeads by thioacetamide leads to CuO–CuS JPs.¹⁵⁶ The same concept was adapted to microgels for creating amide-carboxylic acid Janus microgels, which can be topo-selectively stained with gold NPs.¹⁵⁷ An intrinsic problem is the rotation of the objects at the liquid–liquid interface. Even if several publications report the non-rotation of spherical particles,^{155,156} it seems quite important to find a way to prevent eventual rotation in order to generate APs. In this context, a method involving water in oil emulsions containing different monomers in both phases and modified sub-micrometer silica beads at the interfaces was developed.¹⁵⁸ Upon the polymerisation of both monomers at the particle surfaces, the amphiphilic nature of the particle increases, preventing their rotation.¹⁵⁸ Another approach, using a quite similar system but with an oil in water emulsion and ~100 nm silica beads modified with polymer brushes, has been suggested.¹⁵⁹ It consists of polymerizing not only at the bead surface, but in the whole emulsion, and thus the viscosity is also increased, preventing possible rotation.¹⁵⁹

5.1.2. Polymer and wax-based Pickering emulsions. Another possibility for decreasing the rotation of spherical particles at Pickering interfaces is to literally trap them prior to their toposelective modification. This can be achieved by using oil in water emulsions with droplets containing monomers or polymers that can be respectively hardened through polymerization¹⁶⁰ or solvent evaporation.¹⁶¹ Granick's team developed an efficient and simple technique for the production of large quantities of JPs

(Fig. 4a). A Pickering emulsion is realized with wax droplets in water, stabilized by silica microbeads at a temperature where the wax is liquid. Cooling down the solution solidifies the wax, locking the particles with one wax-protected half (Fig. 4b, inset). A chemical modification is then possible directly through the water phase¹⁶² or by taking out the waxy colloidosomes and modifying them in the vapor-phase (Fig. 4b).¹⁶³ Wax dissolution liberates the APs. Dipolar and amphiphilic JPs with micrometer size were synthesized at the gram scale¹⁶⁴ with ~50% yield.¹⁶² This is not only attractive from a productivity point of view, but the technique is also interesting because it allows a fine control of the “Janus balance” since the particle embedding in the wax phase is easily controllable by parameters such as ionic strength, pH and surfactant addition.¹⁶⁴ Other groups used Granick's process to synthesize micrometer-sized JPs with two sorts of responsive polymers,¹⁶⁵ sub-micrometer sized polymer-laponite core-shell particles with anisotropic surface potentials,¹⁶⁶ and 100 nm silica JPs.¹⁶⁷ Etching of the unprotected silica part leads to original AP morphologies.¹⁶⁸ Kim *et al.* developed an

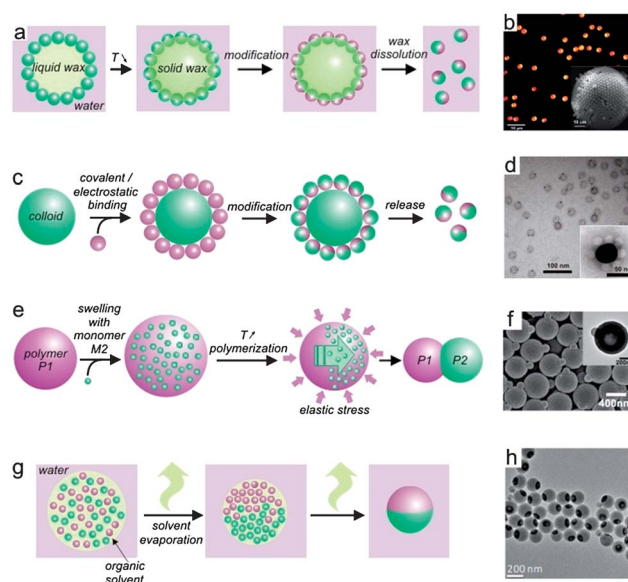


Fig. 4 (a) Scheme of the wax-based Pickering emulsion method. (b) Epifluorescence image of silica Janus beads synthesized by the wax-based Pickering emulsion method. Reprinted with permission from ref. 163 Copyright (2008) American Chemical Society. Inset: scanning electron microscope (SEM) micrograph of a wax colloidosome stabilized with silica particles. Reprinted with permission from ref. 164 Copyright (2008) American Chemical Society. (c) Scheme of the suspension-based techniques for synthesizing APs. (d) TEM micrograph of asymmetric organic NPs synthesized by the cyclic templating strategy, where the thiol modified parts are labeled with gold NPs. Reprinted with permission from ref. 175 Copyright (2011) American Chemical Society. Inset: TEM image of a templating gold NP covalently linked with organic NPs before ligand exchange.¹⁷⁵ (e) Seeded emulsion polymerization scheme. (f) SEM picture of snowman-like polyacrylonitrile–polystyrene particles synthesized by seeded emulsion polymerization. Inset: TEM image of a unique particle. Reprinted with permission from ref. 180 Copyright (2010) American Chemical Society. (g) Scheme of solvent evaporation in the emulsion droplet technique. (h) TEM micrograph of magnetic spherical particles obtained with this technique. Reprinted with permission from ref. 116 Copyright (2010) American Chemical Society.

interesting process which requires a photocurable oil phase in an oil in water Pickering emulsion.¹⁶⁹ The particles are PS microbeads and the droplets contain a photocurable polymer. Using ultrasound treatment, the droplets are divided into smaller entities, and even though the majority exhibits a raspberry-like morphology, some of them form APs, that can be hardened upon UV-curing. The affinity between polymer and PS particles will direct the AP final shape from JPs to snowman-like APPs.¹⁶⁹

5.2. Suspension-based techniques

Adapting the quite simple two-dimensional processes, which can be employed at a solid–liquid interface, to suspensions seems a very good alternative for increasing the surface area, and thus the productivity. In order to increase the accessible surface, the key parameter is a decrease in colloid size. A few processes, even at the nanoscale, are already available, which is very promising for the industrial production of APs.

5.2.1. Breaking the symmetry of micrometer and sub-micrometer particles. Poncet-Legrand *et al.* developed a technique based on the covalent binding of ~ 100 nm silica particles to PMMA and commercial resin microbeads.¹⁷⁰ After successful binding, gold NPs can be adsorbed at one extremity of the silica particles, and finally APs are released from the PMMA or the resin by calcinations or chemical cleavage (Fig. 4c).¹⁷⁰ Several other strategies were developed, based on electrostatic binding of nanometer-sized spherical particles to sub-micrometer sized colloids with opposite surface charges. Negatively charged polymer coated magnetite NPs were adsorbed on positively charged silica beads. The parts screened by the NPs were not affected by the subsequent polymerization and these APs were detached from the beads by changing the silica surface charge through increasing the pH.¹⁷¹ A similar process based on electrostatic adsorption of ~ 100 nm microgels on sub-micrometer PS beads, followed by a radical polymerization and bead dissolution, led to asymmetric polymer-coated microgels.¹⁷² In a totally different approach, Nie *et al.* used hydrophobic-polymer coated yttrium hydroxide nanotubes (NTs). The NTs were suspended in an aqueous solution containing a monomer. A hydrophobic cross-linker and an initiator were located in the hydrophobic coatings of the NTs. The crosslinker polymerizes until reaching the water interface, where the hydrophilic monomer starts polymerizing, forming Janus micelles after dissociation from the NTs.¹⁷³ Finally, Mao *et al.* showed elegantly that the templating particle can also be the modifier. They have designed thiol-terminated oligomers that form micelles in toluene in such a way that the thiol moieties are oriented towards the outside of the micelle. Binding of gold NP on the surface of these few hundreds of nanometers micelles was achieved. After micelle dissociation by the addition of an appropriate solvent, gold NP attached to oligomers in a dissymmetric way are released.¹⁷⁴

5.2.2. Towards nanoparticle surface templating. One very promising process, showing a symmetry break at NP surfaces, was very recently reported by Zhang *et al.* They proposed a cyclic templating strategy based on click chemistry, that involves as templating particles a few tenths of nanometer gold NPs functionalised with alkine ligands attached by thiols and smaller

azide coated hydrophobic organic NPs as substrates to be modified.¹⁷⁵ The cycle consists of (i) binding of the organic NPs to the gold NPs by click chemistry (Fig. 4d, inset), (ii) removal of the excess organic NPs, (iii) ligand exchange at the gold NP interface, which liberates the organic NP, possessing now thiol moieties at one face and (iv) organic APs recovery. The presence of thiols at one extremity of the nanosized APs was demonstrated by their anisotropic binding to 1 nm gold NPs (Fig. 4d).¹⁷⁵ This first report shows that the surface of NPs can be used, based on covalent binding, for breaking the symmetry and predicts important developments in the near future in this area.

6. Emulsions as bulk templates for breaking the symmetry

Many reports have shown that emulsions can be used to break the symmetry by emulsion polymerisation and solvent evaporation. Different strategies based on this technique are currently employed to generate APs leading to a large range of possible combinations with different accessible length scales.

6.1. Seeded emulsion polymerisation

The so-called “seeded emulsion polymerization” (SEP), can lead to homogeneous APs with dumbbell, acorn-like and snowman-like morphologies, but requires multiple steps (Fig. 4e). The classical SEP involves a monomer-swollen polymer as the seed. Basically, the procedure requires three steps, which are (i) polymerisation of a monomer M1 emulsified in water with the help of a surfactant to give polymer P1, (ii) P1 swelling by incorporation of a monomer M2 that creates the “seed”, and (iii) heating and polymerization of the seed. The elastic stress generated by the entropy change during the third step can cause a phase separation between P1 and M2 that will be generally increased during the polymerization of M2, due to the difference of hydrophilicity leading to P2 protrusion, which will generate the AP patch (Fig. 4f). Mock *et al.* investigated the SEP mechanism, highlighting the importance of key parameters such as wetting affinities between M2 and the seed and the swelling time in determining the final particle morphology.¹⁷⁶ SEP and a subsequent site-selective modification were used to synthesize few micrometers,¹⁷⁷ sub-micrometer¹⁷⁸ and ~ 100 nm amphiphilic organic APs¹⁷⁹ as well as sub-micrometer organic–inorganic APs.¹⁸⁰ It is worth mentioning that Kim *et al.* increased the level of structural complexity by introducing a subsequent monomer swelling to dumbbell-like asymmetric particles previously synthesized by SEP, leading, after heating and polymerization, to original trimeric structures.¹⁸¹ By encapsulating in the swollen polymer seed an inorganic core particle, sub-micrometer sized silica/organic APs (Fig. 6a),¹⁸² and magnetic hollow APs were synthesized.¹⁸³ Recently, SEP has been extended and other processes, which do not use a monomer swollen polymer as seeds, can still be found under the name SEP or seeded dispersion polymerization (SDP), when the seeds are particles. A few procedures involving inorganic particles as seeds have been reported in the literature. Styrene emulsion polymerization with silica seeds in the presence of a hydrophilic monomer can lead, by optimizing the monomer-seed ratio, to a few hundreds of nanometers snowman-like APs.¹⁸⁴ The PS part can be used as

a protecting mask that can be dissolved after the modification to leave a “naked” silica area that undergoes subsequent modifications.¹⁸⁵ Styrene emulsion polymerization in the presence of Fe₃O₄–silica core–shell particles coated with a coupling agent as seed can lead to particles coated with a polymeric shell or a bulb, depending on the reticulation degree.¹⁸⁶ Breaking the symmetry of the concentric particles is possible using them as seeds for SEP, leading to ~500 nm snowman-like particles.¹⁸⁶ Organic particles as seeds have also been reported. Using PS beads as seeds, micrometer-sized organic particles can be created.¹⁸⁷ Recently, sub-micrometer sized silica–PMMA core–shell particles, supporting silica particles, were used as seeds to generate original organic–inorganic dumbbell-like APs.¹⁸⁸ Finally, oil droplet seeded emulsion polymerization has been introduced. Using ferromagnetic oil droplets swollen with styrene monomers as seeds, Rahman *et al.* generated ~100 nm acorn-like ferromagnetic APs.¹⁸⁹

6.2. Emulsion droplets as asymmetry inducing polymerization reactors

The one step synthesis of ~100 nm PS–silica snowman-like APs was reported by mini-emulsion polymerization. No seeds are present and the droplets are composed of monomers and TEOS. During the polymerization, that takes place at 70 °C in the presence of ammonia, a spontaneous phase separation occurs.¹⁹⁰ A similar approach based on sonochemistry involves droplets filled with magnetite particles to generate ~50 nm ferromagnetic APs.¹⁹¹ Very original APs were synthesized using wax droplets containing styrene. Upon polymerisation by heating, a phase separation occurs (similarly to SEP) between polystyrene and the droplet, and the polymer is dragged to the interface due to the Pickering effect.¹⁹² A subsequent interfacial polymerization of water soluble monomers breaks the symmetry. Since the PS phase morphology at the interface depends on the cross-linking and the surfactant concentration, very original micrometer APs morphologies were reported.¹⁹² Misra and Urban recently reported the two-step synthesis of ~100 nm acorn-like JPs by emulsion polymerisation.¹⁹³ They showed that this morphology can be obtained by subsequently polymerising two monomers with a similar glass transition temperature that is high enough compared to the reaction temperature. The interfacial energy between the polymers has to be sufficient to favour a phase separation with a restricted contact area.¹⁹³ It has also been reported that immiscible polymers with different molecular weights can phase-separate when incorporated in mini-emulsion droplets.¹⁹⁴

6.3. Solvent evaporation in emulsion droplets

Evaporation of an organic emulsion droplet containing two products can lead to a phase separation since during evaporation the less soluble product will precipitate first while the other concentrates and precipitates when saturation is reached (Fig. 4g). The formation of amphiphilic PS–PMMA APs particles by toluene evaporation has been intensively studied. It has been shown that parameters such as the type of surfactant,¹⁹⁵ the surfactant concentration,^{195,196} and the molecular weight of the polymer,^{196,197} are critical with respect to the APs final

morphologies. By tuning these parameters, one can synthesize micrometer-sized acorn-like APs and snowman-like APs as well as spherical JPs. After having induced the symmetry break with this technique, Tanaka *et al.* used the surface initiated atom transfer radical polymerization to generate micrometer-sized mushroom-like APs.¹⁹⁸ Besides these fully organic systems, inorganic–organic APs can also be created by using this technique. Indeed, hydrophilic magnetite NPs, inserted in droplets with PS or amphiphilic polymer will segregate in the particle during toluene evaporation, forming spherical APs with size-controllable magnetic patches (Fig. 4h).^{116,199} In a quite similar approach, Higuchi and coworkers reported polymer NP formation of THF-soluble diblock copolymers. After being solubilized in a water–THF mixture, the copolymers spontaneously self-assemble upon slow THF evaporation leading to microphase separation and they precipitate.²⁰⁰ Engineering the copolymer molecular weights and the block length allows the final organization to be tuned; long blocks can give ~100 nm spherical JPs.²⁰¹

7. Breaking the symmetry without interfaces

7.1. Polymerization techniques

7.1.1. Polymer protrusion. Polymerization methods other than seeded emulsion polymerization that can produce polymer protrusions have been recently reported. Even if the involved mechanisms are not well understood, suggestions were proposed by the authors. Micrometer-sized PS spheres covered with a polyelectrolyte multilayer (PEM) can exhibit a protrusion of the polymer core in the presence of small amounts of THF, leading to PS–PEM snowman or dumbbell-like APs.²⁰² It has been suggested that due to hole generation in the PEM layer upon the swelling and the osmotic pressure in the presence of THF molecules, the PS core can protrude through the shell and be stabilized by sulfate groups present in the PS latex.²⁰² PS polymerization on ~400 nm vinyl-modified silica beads can also lead to a polymer bulge when the monomer is added dropwise in the presence of low amounts of surfactant.²⁰³ It has been observed that a small bulge forms, and suggested that the slow monomer addition favours its adsorption on the preformed PS, which directed the protrusion growth. Organic–inorganic spherical PPs can be recovered after having etched the thinner PS layer.²⁰³

7.1.2. Polymerization in the presence of nanoparticles. Ohnuma *et al.* reported the formation of PS–gold snowman-like spherical APs with very high yield by simply adding citrate-stabilized gold NPs after the PS precipitation polymerization is initiated (Fig. 5a).²⁰⁴ Even if the symmetry-breaking mechanism is not known, the particle evolution was observed during the reaction and it was found that PS nucleates and grows at the gold NP surface without embedding it. The NPs addition time and the type of NP stabilizing agent seem to be critical parameters.²⁰⁴ It has also been reported that aniline polymerization triggered by AgNO₃ in the presence of gold nanospheres or nanorods leads to PPs with a gold–silver core–shell patch (Fig. 5b).²⁰⁵ Fe₃O₄ nanoparticles can also be partially embedded in a PS matrix, when present during radical emulsion-free styrene

polymerization, to create ~ 100 nm PPs that can be subsequently modified by silica in a dissymmetric fashion (Fig. 5c).²⁰⁶

7.2. Copolymer engineering

Even if some linear diblock copolymers and more sophisticated polymers^{207–209} with rather small molar masses can exhibit an intrinsic Janus character, bigger objects, that can be easily manipulated, are also required in the frame of nanotechnology. Those nanometric objects can be obtained through the following different techniques.

7.2.1. Comb-like copolymers and intramolecular cross-linkage. High molar mass comb-like copolymers can form unimolecular asymmetric nano-objects with different asymmetric morphologies.^{210,211} For example, Lanson *et al.* showed that poly(styrene) comb-poly(ethylene oxide) copolymers form 100 nm long cylindrical structures with both domains easily observable under the atomic force microscope (AFM) (Fig. 6b).²¹⁰ Cheng *et al.* reported the synthesis of the “smallest” polymeric PP by cross-linking the internal part of a triblock copolymer leading to ~ 10 nm APPs with two asymmetric polymer chains as patches.²¹²

7.2.2. Techniques based on block-copolymer self-assembly. AP synthesis by copolymer self-assembly has a strong potential for industrial applications because of its cheapness, simplicity and the small size of APs that can be produced. Janus micelles can be created by simply mixing block copolymers that will self-assemble. Voets *et al.* reported that the bulk self-assembly of two diblock copolymers can lead to ~ 20 nm-sized Janus disks,²¹⁴ and ellipsoidal Janus objects.²¹⁵ A precise transmission electronic microscope (TEM) observation of these polymeric Janus micelles still remains a challenge, that can be overcome by staining them for example with Grubbs catalyst²¹⁶ or by the topologically catalyzed modification with a silica precursor.²¹⁷ In some cases the sole self-assembly is not efficient and a subsequent annealing,²¹⁸ photo-crosslinking²¹⁹ or intramolecular complexation²²⁰ is required to break the symmetry. Li *et al.* recently reported the synthesis of vesicles by diblock copolymer self-assembly in the presence of HCl or hydrogen tetrachloroaurate. The

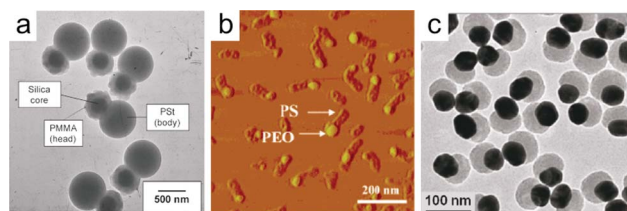


Fig. 6 (a) TEM image of asymmetric dumbbells composed of a PMMA coated silica head and a PS body. Reprinted with permission from ref. 183 Copyright (2010) American Chemical Society. (b) Topographic AFM tapping mode image of asymmetric polymeric objects exhibiting PS and PEO domains. Reprinted with permission from ref. 210 Copyright (2007) American Chemical Society. (c) TEM picture of gold-SiO₂ APs obtained by ligand segregation. Reprinted with permission from ref. 213 Copyright (2010) American Chemical Society.

dissociation of these vesicles by hydrazine addition leads to nanometer-sized asymmetric fully organic or mixed organic–gold PPs.²²¹ A very original method was recently reported by Dupont *et al.* After the precipitation of one of the external blocks of a triblock copolymer by addition of a complexing agent, the polymers self-assemble in a hamburger-like way with insoluble “bun” parts and a “filling” middle block.²²² After the bun parts were photo-crosslinked, the removal of the complexing agent leads to an opening of the sandwich, creating two nanometer-sized Janus particles.²²² It is well known that triblock copolymers can self-assemble in bulk lamellar structures that are different, depending on the block sizes and the solvent used (Fig. 7a).

Saito *et al.* first reported the use of the lamellae-sphere structure formed by A–B–C triblock copolymers with spheres of block B embedded between lamellae outer blocks of A and C, for synthesizing ~ 20 nm spherical Janus micelles after crosslinking of the B spheres.²²³ Müller’s team, about the same time, reported the use of the same technique for creating Janus micelles with other compositions (Fig. 7b).^{224,225} This team then extended the technique, demonstrating the wide range of possible shapes. The usual route consists in selectively crosslinking a bulk film block terpolymer with a subsequent sonication treatment. By cross-linking cylinders in lamellae-cylinder morphologies, they could obtain micrometer-long Janus cylinders (Fig. 7c).²²⁶ Finally, the lamellae–lamellae morphology allowed them to synthesize Janus disks with tuneable sizes (Fig. 7d).²²⁷

7.3. Towards a growth control of patches on silica particles

After having shown that silver patches on ~ 300 nm silica beads could be grown with a control over their number and morphologies leading to PPs and JPs with a two-step technique,²²⁸ Klupp Taylor’s group reported an attractive one step process.²²⁹ The strategy is based on generating statistically very few nucleation events per silica bead by using small concentrations of silver salt and a slow dropwise addition of reducing agent (Fig. 8a).²²⁸ The importance of reaction temperature and type of silica nanobeads was investigated.²²⁹ The number of particles owning only one patch is very high and the modification yield can be very close to 100% using optimized parameters.²²⁹ In addition to its direct potential interest for industrial production of silver PPs, this technique may open new opportunities for

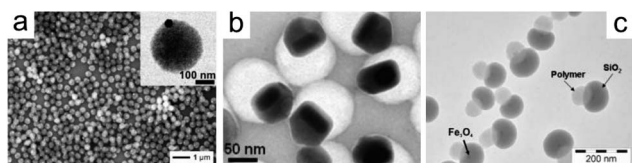


Fig. 5 (a) Scanning electron microscope (SEM) image of PS-gold PPs obtained by polymerization in the presence of gold NPs. Inset: TEM picture of a unique PS-gold PP. Reprinted with permission from ref. 204 Copyright (2009) American Chemical Society. (b) TEM micrograph of APs containing a gold-silver core-shell particle and a spherical polyaniline part obtained by aniline polymerization with AgNO₃ in the presence of gold nanorods. Reprinted with permission from ref. 205 Copyright (2010) American Chemical Society. (c) TEM picture of mushroom-like PS-SiO₂ APs with an embedded Fe₃O₄ NP. Reprinted with permission from ref. 206 Copyright (2010) American Chemical Society.

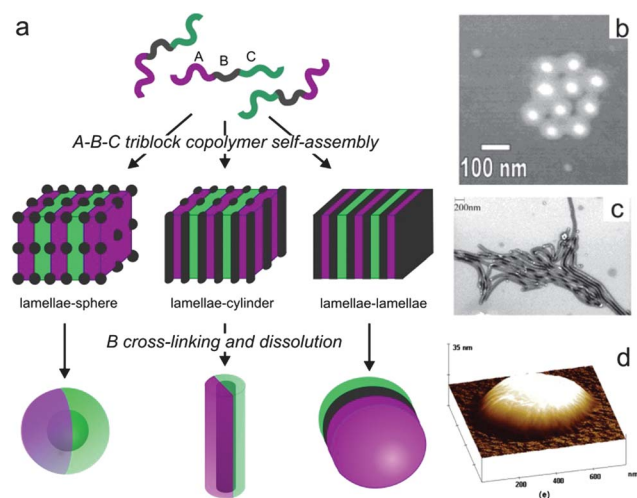


Fig. 7 (a) Scheme of the synthesis pathway based on triblock copolymer self-assemblies developed by Müller's group⁴ for synthesizing Janus spheres, Janus cylinders and Janus disks. (b) Surface force microscopy (SFM) image of an assembly of spherical Janus micelles. Reprinted with permission from ref. 224 Copyright (2001) American Chemical Society. (c) SEM images of Janus cylinders. Reprinted with permission from ref. 226 Copyright (2003) American Chemical Society. (d) 3D-plotted SFM image of a Janus disk. Reprinted with permission from ref. 227 Copyright (2007) American Chemical Society.

creating other APs, since adapting it to other systems seems quite straightforward.

7.4. Core-shell and hollow particles as sources of asymmetry

7.4.1. "Out of the shell" pathway. Two examples were reported with core-shell particles as sources of APs. They are based on chemical or crystalline transformation that imply volume changes of the core or the shell part in such a way that the core cannot remain anymore in the shell. Formation of AgI-silica nanometer-sized snowman-like PPs using Ag-silica core-shell nanospheres under I_2 action was observed with TEM (Fig. 8b).²³⁰ I_2 diffuses through the nanoporous silica and oxidizes Ag^0 into AgI. The differences in molar volumes between the two silver compounds make AgI leave the shell, leading to an AgI bulb outside the shell, linked to the core part by a filament. Dewetting of a CdSe shell caused by a change from amorphous to crystalline upon annealing can induce a FePt core to leave the shell forming FePt-CdSe snowman-like nanometer PPs (Fig. 8c).²³¹ The protrusion of the PS core of PS-PEM core-shell particles in certain solvents was also reported by Wang *et al.*²³²

7.4.2. Janus sheets by crushing hollow spheres. Even if it is difficult to imagine a precise size control of the generated particles using this technique, crushing hollow spheres with a modified outer-surface is a very easy and attractive way for generating Janus objects, as was mentioned by de Gennes (Fig. 8d).² The first description of this strategy goes back to a 1987 patent from Grüning *et al.* describing the formation of Janus microplates by crushing commercial hollow silica microspheres that have a hydrophobic modified outer surface.²³³ Recently, this technique has been adapted to lab-made²³⁴ hollow silica microspheres to generate paramagnetic Janus sheets.³⁸

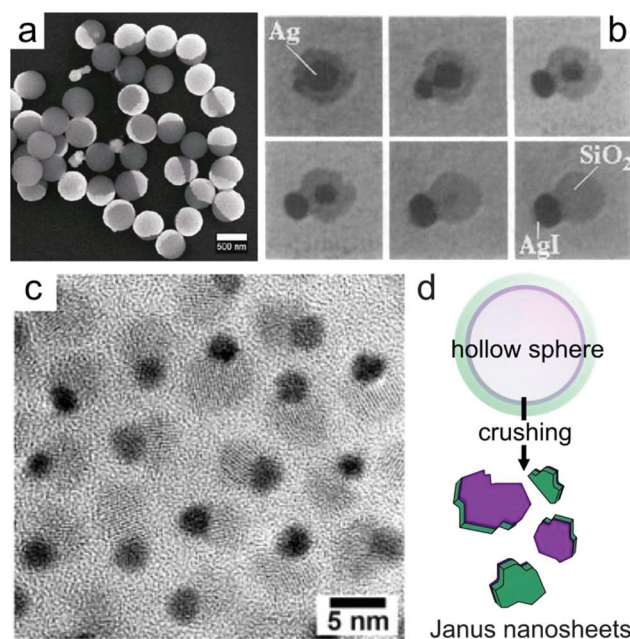


Fig. 8 (a) SEM image of silica-gold PPs obtained by the method reported by Klupp Taylor. Reprinted with permission from ref. 228 Copyright (2010) American Chemical Society. (b) TEM micrographs showing the transformation of a Ag-SiO₂ core-shell particle in an AgI-SiO₂ snowman-like AP under the I_2 action, the core diameter is 9 nm. Reprinted with permission from ref. 230. (c) FePt-CdSe snowman-like PPs obtained by annealing of FePt-CdSe core-shell NPs. Reprinted with permission from ref. 231 Copyright (2004) American Chemical Society. (d) Scheme showing the formation of Janus nanosheets by crushing hollow spheres.

7.5. Janus vesicles

By dialyzing a solution containing vesicles with phosphatidylcholine lipid membranes, detergent and dodecane-thiol stabilized gold nanoparticles, Rash *et al.* formed Janus vesicles. Indeed, the detergent removal caused, by dialysis forces, the NPs to migrate to the inner lipid bilayer, then, hydrophilic attraction between the gold NPs causes their segregation within the membrane, leading to new, very interesting Janus nanovesicles, that have a strong potential for targeted drug delivery.²³⁵ Christian *et al.* showed that the addition of a binding cation to vesicles composed of a neutral and an anionic amphiphilic polymer can lead to a phase separation, generating Janus vesicles.²³⁶

7.6. Ligand segregation on nanoparticles

Ligand segregation as the origin of symmetry break on gold NP was reported by Chen's group. They showed that some combinations of hydrophobic and hydrophilic gold ligands can segregate at the NP surface, generating two areas with different hydrophilicities on the NP surface.^{213,237,238} The symmetry is then broken and subsequent modification can lead to APs composed of different materials. The adsorption of amphiphilic diblock copolymers on the hydrophilic part can lead to nanometer-sized organic²³⁸ or silica^{213,237} particles with gold patches (Fig. 6c). The degree of embedding of gold NPs in the polymer part can be tuned *via* the hydrophobic ligand-hydrophilic ligand ratio.²¹³

Taking advantage of the segregated adsorption of mercapto-benzoic acid and polyacrylic acid around gold NPs, silica growth with tetraorthosilicate precursors was only achieved at the hydrophilic NP half to form snowman-like APs.²³⁸

7.7. Mechanisms for toposelective modification of metallic or semiconductor nanoparticles

7.7.1. Selective deposition on nanorod tips. Most of the time, the tips and the core surface of anisotropic metallic or semi-conducting (SC) nanostructures exhibit reactivity differences. This is mainly due to the different exposed crystal facets. Usually, tips present higher surface energies than core surfaces and also imperfections of the stabilizing ligand layer. This decreases the activation energy for a particle to nucleate at a tip site, followed by the autocatalytic growth of the initially deposited particle. Taking advantage of this phenomenon and the fact that on CdSe or CdS nanorods the tip facets present more chalcogenide atoms compared to the core surface (thus, higher affinities for metals), Pt, PtNi and PtCo particles have been selectively deposited at the tip of ~120 nm long CdS nanorods.²³⁹ In some cases, the amount of metal precursor modifies the final morphology. Statistically, smaller concentrations will give a modification only at one tip and increasing the concentration will favour metal NPs at both tips.²³⁹ Using this mechanism, CdS nanorods with one PbSe extremity,²⁴⁰ CdSe-seeded CdS nanorods with one Co extremity (Fig. 9a),²⁴¹ one gold extremity,²⁴² one Ag₂S extremity,²⁴³ and, at the same time, one gold and one Ag₂S tip were synthesized.²⁴² Toposelective modification with gold was also reported on bullet-shaped CdS nanocrystals, generating original PPs.²⁴³ Other nanorods than CdS or CdSe have been employed and the selective modification of one tip were reported for TiO₂ nanorods with Fe₂O₃²⁴⁴ and Co,²⁴⁵ ZnO nanowires with TiO₂,²⁴⁶ Te nanowires with gold (Fig. 9b),²⁴⁷ Pt and FePt nanowires with gold²⁴⁸ and Co nanorods with gold.²⁴⁹

7.7.2. Asymmetric particles by the Oswald-ripening mechanism. After having introduced for the first time the gold deposition on CdSe nanorods to generate dumbbell-like nanostructures,²⁵¹ Mokari *et al.* have shown experimentally and theoretically that by increasing the gold precursor concentration, a matchstick-like morphology with the gold being deposited only at one nanorod tip appears.²⁵⁰ This phenomenon, observed for rods with a few tenths of nanometers and ~10 nm CdSe dots was

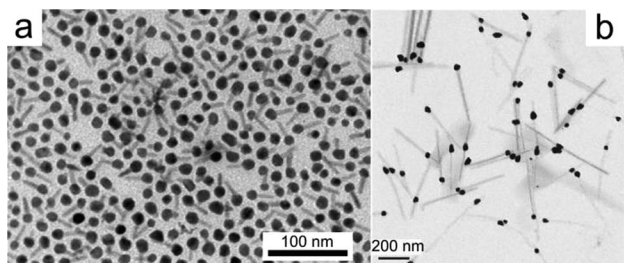


Fig. 9 (a) TEM picture of Co-tipped CdS nanorods. Reprinted with permission from ref. 241 Copyright (2009) American Chemical Society. (b) TEM image of Te nanowires with gold tips. Reprinted with permission from ref. 247 Copyright (2009) American Chemical Society.

explained by an Oswald-ripening mechanism. Indeed, at high gold precursor concentrations, the gold density fluctuation provides sufficient driving force for a ripening, where the smaller gold dots, being destabilized compared to the bigger ones, are consumed, while the size of the bigger ones increases, leading to nanometer-sized SC-metal matchstick-like APs and JPs. This dissolution-deposition mechanism implies an electron transfer that was suggested to occur by hopping through surface states.²⁵⁰ This ripening mechanism was also used to generate nanometer-sized CdS matchstick-like APs with gold at one extremity²⁵² and Fe₃O₄-Ag PPs.²⁵³

7.7.3. Surface energy balance. Seh *et al.* studied TiO₂ growth on gold nanorods and nanospheres.²⁵⁴ Various morphologies were obtained by using different TiO₂ precursor amounts, which in some cases allowed formation of ~50 nm snowman-like and nanometer-sized TiO₂ spheres containing a partially embedded gold nanorod.²⁵⁴ The authors rationalized their formation with a model based on the balance between the gold surface energy, TiO₂ surface energy and the gold-TiO₂ interfacial energy. Indeed, for some TiO₂ precursor volumes, the more stable morphologies were found to be the asymmetric ones.²⁵⁴

7.7.4. Lattice mismatch. γ -Fe₂O₃-metal sulfide NP morphologies were investigated by Kwon *et al.* Their synthetic pathway consisted in annealing γ -Fe₂O₃-metal sulfide core-shell particles, which induced a rearrangement of the metal sulfide shell, creating crystalline NPs with heterojunctions.²⁵⁵ Studying metal sulfides with different lattice parameters, they pointed out the importance of the lattice mismatch between the two materials for the final morphology.²⁵⁵ Indeed, the two extreme effects of inappropriate mismatch will be generation of separated particles or multipatches and cluster formation. A right balance can be found with systems such as γ -Fe₂O₃-CdSe nanometer-sized PPs.²⁵⁵ The authors then studied the influence of the Fe₂O₃ nanocrystal size on the final morphology.²⁵⁶ By using a cation exchange procedure for CdS nanocrystals, Saruyama *et al.* reported the formation of CdS-CdTe PPs. The anisotropic nucleation of CdTe on CdS was also explained by lattice mismatch and a difference between the crystal structures of the two materials.²⁵⁷

7.7.5. Metal sulfides anisotropic growth. A process for generating metal-sulfide PPs has been reported by Teranishi and co-workers.¹⁹ The method consists of growing first metal NPs protected by thioalkanes ligands. At high temperature, some S-C bonds are broken, incorporating some sulfur atoms in the metal. In the presence of another metal precursor, the new metal sulfide grows anisotropically, probably in a direction favoured by the transport of S²⁻ ions from the metal sulfide previously created. Using the technique, PdS_x-Co₉S₈²⁵⁸ nanoacorns, as well as CdS-PdS_x PPs²⁵⁹ and copper-indium sulfide PPs²⁶⁰ were reported.

7.7.6. Growth from a single facet. Yu *et al.* reported the formation of Fe₃O₄-gold snowman-like nanostructures by decomposition and oxidation of Fe(CO)₅ in the presence of spherical gold NPs.²⁶¹ The proposed mechanism is due to the charge polarization at the gold-Fe₃O₄ interface when Fe₃O₄

begins to nucleate at one facet. The other facets then become electron deficient, protecting them from other nucleation events.²⁶¹ The obtained APs are approximately of 10 nm size with easily tuneable patches²⁶¹ and can serve as platforms for growing other materials from the gold patch.²⁶² Shi *et al.* extended the method by synthesizing Fe₃O₄ and PbS NPs with gold patches and Fe₃O₄-Au-PbS APs using this technique.²⁶² Pellegrino *et al.* grew epitaxially gold on CoPt₃ nanocrystals, creating nanometer-sized APs.²⁶³ The proposed mechanism implies the selective nucleation of gold on a single facet, making this facet catalytically active with respect to the further growth of CoPt₃.²⁶³ Involving the same mechanism, ZnO-gold snowman-like nanostructures were synthesized.²⁶⁴ Synthesis of nanometer-sized FePt-CoFe₂O₄,²⁶⁵ Ag-Se,²⁶⁶ FePt-Au,²⁶⁰ Ag₂S-ZnS,²⁶⁷ Ag₂S-CdS,²⁶⁷ Fe₃O₄-SiO₂,²⁶⁸ and FePt-Au²⁴⁸ APs probably implies one of the two mechanisms mentioned above.

7.8. Flame synthesis approach

A flame synthesis approach was proposed by Zhao and Gao.²⁶⁹ In their device, a solution containing Fe₂O₃ and silica precursor is injected into a flame, the reaction is then quenched and the resulting NPs are collected in a thin water layer generated on a rotating disk. They found out that the resulting particles were nanosized spherical SiO₂-Fe₃O₄ JPs. They explained their formation by solvent evaporation, followed by a phase separation in the liquid state during pyrolysis. Even if the production rate was rather low, this technique seems well adapted for up-scaling.²⁶⁹

7.9. Approaches using external electromagnetic fields

The polarization of SC or conducting objects that can be generated under the influence of electromagnetic fields such as radio-frequencies,²⁷⁰ micro-waves,²⁷¹ light²⁷⁰ and electric fields²⁷² can trigger their toposelective modification. We now discuss the case of selective modification for generating APs based on these kinds of effects.

7.9.1. Photochemistry. Light absorption by SC materials can promote electrons from their valence band to the conduction band. Even if the recombination rate is most of the time very important, the photogenerated hole and electron can react with electron donors and acceptors respectively. Some cases of located deposition on SC particles upon irradiation with light leading to APs can be found in literature. Reiche *et al.* showed that dark areas of illuminated TiO₂ particles can be the place for Cu²⁺ reduction, while the light exposed area is an oxidation site.²⁷³ SC nanorods were also selectively modified with metals upon light exposure. The single tip modification of ZnO nanorods with silver,²⁷⁴ and of CdS nanorods with gold, have been reported.^{275,276} Even if the single-tip modification mechanism is still unclear, it has been suggested that once a metal nuclei is created at one of the tips (due to preferential deposition compared to the body surface, as discussed above), the metal, due to its large capacitance attracts the photoinduced electrons for the growth of the rest of the metal NP.

7.9.2. Bipolar electrochemistry. Bipolar electrochemistry is based on the polarization of conductive objects in DC electric

fields.^{272,277} Indeed, the electric field induces a polarization potential difference equal to the electric field multiplied by the object length, which arises between the two sides of the object, creating a cathodic and an anodic pole, which constitutes the driving force that can be used to trigger depositions (Fig. 10a). Bradley *et al.* used this technique to deposit Pd^{278–280} and a conducting polymer²⁸¹ on carbon microstructures, but since the particles were adsorbed on sheets before their modification during the experiment, this technique cannot be considered as a bulk synthesis. With the capillary assisted bipolar electrodeposition (CABED) a bulk technique for achieving bipolar electrodeposition has been suggested.²⁸² This set-up allows applying the high electric fields (~ 1500 V cm⁻¹) that are required for modifying small objects. A family of asymmetric metal coated carbon microtubes could be generated^{76,84} (Fig. 10b and c) by combining a metal deposition at the cathodic pole, accompanied by solvent oxidation at the anodic pole (Fig. 10a). This concept could be extended also to polymer-carbon-metal APs²⁸³ and it is possible to use the technique at the nanoscale, as has been demonstrated for multiwall carbon nanotubes (MWCNT) with a single gold NP at one tip (Fig. 10d).²⁸² Even if this is a bulk technique, the accessible amount of APs is limited by the capillary volume. Since this technique is attractive, because it seems very appropriate for an industrial AP production, work is under progress to upscale the technique for reaching gram-scale production.²⁸⁴

7.9.3. Microwaves and radio frequencies induced polarization. Duque *et al.* deposited metals at surfactant coated single-wall carbon nanotube (SWCNT) tips by exposing them, in the

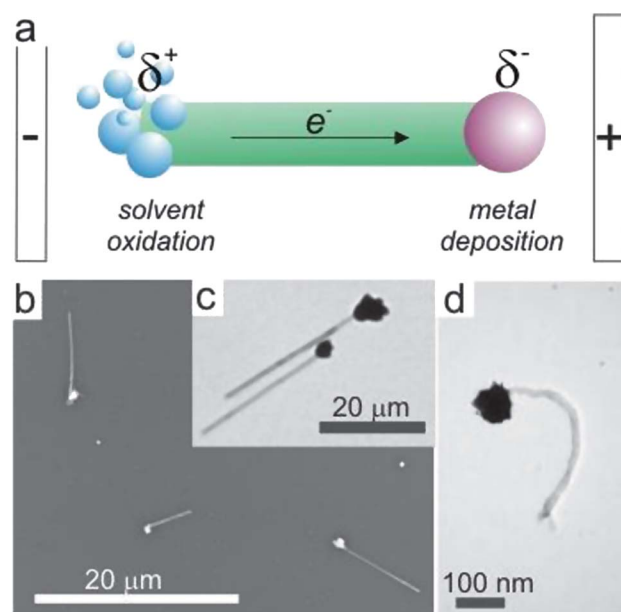


Fig. 10 (a) Scheme of the bipolar electrodeposition of a metal at one end of a conducting tube. (b) SEM image of carbon microtubes modified by bipolar electrochemistry with Pt particles at one extremity.⁸⁴ (c) Optical microscope image of carbon microtubes modified by copper at one extremity by bipolar electrodeposition. Reprinted with permission from ref. 282 Copyright (2008) American Chemical Society. (d) TEM picture of an asymmetric MWCNT modified with a gold NP.

presence of metal salts, to microwaves²⁷¹ and radio-frequencies.²⁷⁰ Indeed, similar to the bipolar electrochemistry approach, under the influence of these fields, the SWCNTs are affected by polarization, which causes their modification. This approach seems also very attractive for the bulk formation of APs, even if a precise control of the obtained particle morphology has not been clearly demonstrated.

8. Conclusion

Janus and asymmetric particles are of major importance for a wide variety of industrial applications ranging from particulate surfactants to medical treatments. Since the first work related to their synthesis was published in 1988,¹ a very wide range of processes has been developed to produce them, trying to increase the possible material combinations and the amounts of generated APs. Numerous low-dimensional techniques involving interfaces exist and are sufficiently efficient for laboratory scale production, but cannot be considered for a potential industrial scale-up, unless they present a very high yield. In the present contribution, we reviewed the available bulk techniques for AP generation with an accent on their potential practical importance. More fundamental issues, aiming at understanding the mechanisms of symmetry breaking, are equally important²⁸⁵ and need to be taken into account in order to improve the efficiency of these processes. The reviewed approaches consist essentially of creating interfaces in the bulk, using emulsions as templates, polymer engineering, crystal growth engineering and exposing particles to electromagnetic fields. We illustrated the diversity in size, shape and composition that can be obtained with these bulk techniques. Gram-scale production of APs has been reached with relatively good yields by a few groups^{164,4} showing that commercialization of some APs is about to be reached. Nevertheless, the need for adaptable techniques, which can be used to break the symmetry of various types of particles, is still very strong. Obviously, one process will not have the monopoly and several techniques will be used in synergy to reach this diversity. In this perspective, polymer-based techniques and wax-based emulsions seem to be very promising for achieving the production of fully organic, inorganic-inorganic or inorganic-organic APPs. Coupling these relatively well-developed processes with emerging techniques involving external electromagnetic fields, such as in bipolar electrodeposition, can increase the diversity and will finally allow the modification of any kind of particle, with the possibility of a rational design of complex objects at the micro- and nanoscale.

Acknowledgements

This work is partly funded by the CUBIHOLE project, European NanoSci-Era+ action under contract ANR-08-NSCI-008-01 and has also been supported by the French Ministry of Research (MESR), CNRS, and ENSCBP.

Notes and references

- C. Casagrande and M. Veysié, *C. R. Acad. Sci., Ser. II: Mec., Phys., Chim., Sci. Terre Univers*, 1988, **306**, 1423–1425.
- P. G. De Gennes, *Rev. Mod. Phys.*, 1992, **64**, 645–648.
- A. Perro, S. Reculosa, S. Ravaine, E. Bourgeat-Lami and E. Duguet, *J. Mater. Chem.*, 2005, **15**, 3745–3760.
- A. Walther and A. H. E. Müller, *Soft Matter*, 2008, **4**, 663–668.
- M. B. Linder, *Curr. Opin. Colloid Interface Sci.*, 2009, **14**, 356–363.
- X. L. Zhang, J. Penfold, R. K. Thomas, I. M. Tucker, J. T. Petkov, J. Bent, A. Cox and R. A. Campbell, *Langmuir*, 2011, **27**, 11316–11323.
- E. S. Basheva, P. A. Kralchevsky, N. C. Christov, K. D. Danov, S. D. Stoyanov, T. B. J. Blijdenstein, H.-J. Kim, E. G. Pelan and A. Lips, *Langmuir*, 2011, **27**, 2382–2392.
- A.-M. Caminade, R. Laurent, B. Delavaux-Nicot and J.-P. Majoral, *New J. Chem.*, 2012, **36**, 217–226.
- Y. Liu, G. Zhang, L. Niu, L. Gan and D. Liang, *J. Mater. Chem.*, 2011, **21**, 14864–14868.
- S. C. Glotzer and M. J. Solomon, *Nat. Mater.*, 2007, **6**, 557–562.
- J. Du and R. K. O'Reilly, *Chem. Soc. Rev.*, 2011, **40**, 2402–2416.
- A. Perro, E. Duguet, O. Lambert, J.-C. Taveau, E. Bourgeat-Lami and S. Ravaine, *Angew. Chem., Int. Ed.*, 2009, **48**, 361–365.
- A. B. Pawar and I. Kretzschmar, *Macromol. Rapid Commun.*, 2010, **31**, 150–168.
- S. Kudara, L. Carbone, E. Carlino, R. Cingolani, P. D. Cozzoli and L. Manna, *Phys. E.*, 2007, **37**, 128–133.
- M. Yoshida and J. Lahann, *ACS Nano*, 2008, **2**, 1101–1107.
- P. D. Cozzoli, T. Pellegrino and L. Manna, *Chem. Soc. Rev.*, 2006, **35**, 1195–1208.
- S.-M. Yang, S.-H. Kim, J.-M. Lim and G.-R. Yi, *J. Mater. Chem.*, 2008, **18**, 2177–2190.
- M. Casavola, R. Buonsanti, G. Caputo and P. D. Cozzoli, *Eur. J. Inorg. Chem.*, 2008, **2008**, 837–854.
- T. Teranishi, M. Saruyama and M. Kanehara, *Nanoscale*, 2009, **1**, 225–228.
- F. Wurm and A. F. M. Kilbinger, *Angew. Chem., Int. Ed.*, 2009, **48**, 8412–8421.
- Z. Mao, H. Xu and D. Wang, *Adv. Funct. Mater.*, 2010, **20**, 1053–1074.
- S. Jiang, Q. Chen, M. Tripathy, E. Luijten, K. S. Schweizer and S. Granick, *Adv. Mater.*, 2010, **22**, 1060–1071.
- Z. Niu, J. He, T. P. Russell and Q. Wang, *Angew. Chem., Int. Ed.*, 2010, **49**, 10052–10066.
- K. J. Lee, J. Yoon and J. Lahann, *Curr. Opin. Colloid Interface Sci.*, 2010, **16**, 195–202.
- H. Xu, R. Erhardt, V. Abetz, A. H. E. Müller and W. A. Goedel, *Langmuir*, 2001, **17**, 6787–6793.
- B. P. Binks and P. D. I. Fletcher, *Langmuir*, 2001, **17**, 4708–4710.
- Y. Nonomura, S. Komura and K. Tsujii, *Langmuir*, 2004, **20**, 11821–11823.
- S. Jiang and S. Granick, *J. Chem. Phys.*, 2007, **127**, 161102.
- Y. Hirose, *J. Chem. Phys.*, 2007, **127**, 054707.
- T. M. Ruhland, A. H. Gröschel, A. Walther and A. H. E. Müller, *Langmuir*, 2011, **27**, 9807–9814.
- B. J. Park, T. Brugarolas and D. Lee, *Soft Matter*, 2011, **7**, 6413–6417.
- D. J. Adams, S. Adams, J. Melrose and A. C. Weaver, *Colloids Surf., A*, 2008, **317**, 360–365.
- D. L. Cheung and S. A. F. Bon, *Soft Matter*, 2009, **5**, 3969–3976.
- N. Glaser, D. J. Adams, A. Böker and G. Krausch, *Langmuir*, 2006, **22**, 5227–5229.
- Y. K. Takahara, S. Ikeda, S. Ishino, K. Tachi, K. Ikeue, T. Sakata, T. Hasegawa, H. Mori, M. Matsumura and B. Ohtani, *J. Am. Chem. Soc.*, 2005, **127**, 6271–6275.
- J.-W. Kim, D. Lee, H. C. Shum and D. A. Weitz, *Adv. Mater.*, 2008, **20**, 3239–3243.
- T. Tanaka, M. Okayama, H. Minami and M. Okubo, *Langmuir*, 2010, **26**, 11732–11736.
- F. Liang, K. Shen, X. Qu, C. Zhang, Q. Wang, J. Li, J. Liu and Z. Yang, *Angew. Chem. Int. Ed.*, 2011, **50**, 2379–2382.
- D. J. Cole-Hamilton, *Science*, 2010, **327**, 41–42.
- S. Crossley, J. Faria, M. Shen and D. E. Resasco, *Science*, 2010, **327**, 68–72.
- A. Walther, M. Hoffmann and A. H. E. Müller, *Angew. Chem., Int. Ed.*, 2008, **47**, 711–714.
- L.-T. Yan, N. Popp, S.-K. Ghosh and A. Böker, *ACS Nano*, 2010, **4**, 913–920.
- N. Virgilio and B. D. Favis, *Macromolecules*, 2011, **44**, 5850–5856.
- S. Berger, L. Ionov and A. Synytska, *Adv. Funct. Mater.*, 2011, **21**, 2338–2344.
- S.-H. Kim, S. Y. Lee and S.-M. Yang, *Angew. Chem., Int. Ed.*, 2010, **49**, 2535–2538.

- 46 A. Synytska, R. Khanum, L. Ionov, C. Cherif and C. Bellmann, *ACS Appl. Mater. Interfaces*, 2011, **3**, 1216–1220.
- 47 A. Alexeev, W. E. Uspal and A. C. Balazs, *ACS Nano*, 2008, **2**, 1117–1122.
- 48 S. Park, J.-H. Lim, S.-W. Chung and C. A. Mirkin, *Science*, 2004, **303**, 348–351.
- 49 A. Walther, M. Drechsler, S. Rosenfeldt, L. Harnau, M. Ballauff, V. Abetz and A. H. E. Müller, *J. Am. Chem. Soc.*, 2009, **131**, 4720–4728.
- 50 A. G. Vanakaras, *Langmuir*, 2005, **22**, 88–93.
- 51 L. Hong, A. Cacciuto, E. Luijten and S. Granick, *Nano Lett.*, 2006, **6**, 2510–2514.
- 52 L. Hong, A. Cacciuto, E. Luijten and S. Granick, *Langmuir*, 2008, **24**, 621–625.
- 53 Q. Chen, J. K. Whitmer, S. Jiang, S. C. Bae, E. Luijten and S. Granick, *Science*, 2011, **331**, 199–202.
- 54 B. Comiskey, J. D. Albert, H. Yoshizawa and J. Jacobson, *Nature*, 1998, **394**, 253–255.
- 55 H. Takei and N. Shimizu, *Langmuir*, 1997, **13**, 1865–1868.
- 56 J. M. Crowley, N. K. Sheridan and L. Romano, *J. Electroanal. Chem.*, 2002, **55**, 247–259.
- 57 T. Nisisako, T. Torii, T. Takahashi and Y. Takizawa, *Adv. Mater.*, 2006, **18**, 1152–1156.
- 58 S.-H. Kim, S.-J. Jeon, W. C. Jeong, H. S. Park and S.-M. Yang, *Adv. Mater.*, 2008, **20**, 4129–4134.
- 59 S.-N. Yin, C.-F. Wang, Z.-Y. Yu, J. Wang, S.-S. Liu and S. Chen, *Adv. Mater.*, 2011, **23**, 2915–2919.
- 60 O. D. Velev, S. Gangwal and D. N. Petsev, *Annu. Rep. Prog. Chem., Sect. C*, 2009, **105**, 213–246.
- 61 M. Bazant and T. Squires, *Phys. Rev. Lett.*, 2004, **92**, 066101.
- 62 T. M. Squires and M. Z. Bazant, *J. Fluid Mech.*, 2006, **560**, 65–101.
- 63 S. Gangwal, O. J. Cayre, M. Z. Bazant and O. D. Velev, *Phys. Rev. Lett.*, 2008, **100**, 058302.
- 64 S. Gangwal, O. J. Cayre and O. D. Velev, *Langmuir*, 2008, **24**, 13312–13320.
- 65 S. K. Smoukov, S. Gangwal, M. Marquez and O. D. Velev, *Soft Matter*, 2009, **5**, 1285–1292.
- 66 S. Park, S.-W. Chung and C. A. Mirkin, *J. Am. Chem. Soc.*, 2004, **126**, 11772–11773.
- 67 S. T. Chang, V. N. Paunov, D. N. Petsev and O. D. Velev, *Nat. Mater.*, 2007, **6**, 235–240.
- 68 P. Calvo-Marzal, S. Sattayasamitsathit, S. Balasubramanian, J. R. Windmiller, C. Dao and J. Wang, *Chem. Commun.*, 2010, **46**, 1623–1624.
- 69 R. M. Erb, N. J. Jenness, R. L. Clark and B. B. Yellen, *Adv. Mater.*, 2009, **21**, 4825–4829.
- 70 F. S. Merkt, A. Erbe and P. Leiderer, *New J. Phys.*, 2006, **8**, 216.
- 71 H.-R. Jiang, N. Yoshinaga and M. Sano, *Phys. Rev. Lett.*, 2010, **105**, 268302.
- 72 D. Kagan, R. Laocharoensuk, M. Zimmerman, C. Clawson, S. Balasubramanian, D. Kang, D. Bishop, S. Sattayasamitsathit, L. Zhang and J. Wang, *Small*, 2010, **6**, 2741–2747.
- 73 J. Wu, S. Balasubramanian, D. Kagan, K. M. Manesh, S. Campuzano and J. Wang, *Nat. Commun.*, 2010, **1**, 36.
- 74 S. Balasubramanian, D. Kagan, C.-M. Jack Hu, S. Campuzano, M. J. Lobo-Castañón, N. Lim, D. Y. Kang, M. Zimmerman, L. Zhang and J. Wang, *Angew. Chem., Int. Ed.*, 2011, **50**, 4023.
- 75 K. M. Manesh, S. Balasubramanian and J. Wang, *Chem. Commun.*, 2010, **46**, 5704–5706.
- 76 G. Loget, G. Larcade, V. Lapeyre, P. Garrigue, C. Warakulwit, J. Limtrakul, M. H. Delville, V. Ravaine and A. Kuhn, *Electrochim. Acta*, 2010, **55**, 8116–8120.
- 77 P. Tierno, R. Golestanian, I. Pagonabarraga and F. Sagués, *J. Phys. Chem. B*, 2008, **112**, 16525–16528.
- 78 W. Gao, S. Sattayasamitsathit, K. M. Manesh, D. Weihs and J. Wang, *J. Am. Chem. Soc.*, 2010, **132**, 14403–14405.
- 79 O. S. Pak, W. Gao, J. Wang and E. Lauga, *Soft Matter*, 2011, **7**, 8169–8181.
- 80 N. Mano and A. Heller, *J. Am. Chem. Soc.*, 2005, **127**, 11574–11576.
- 81 C. Stock, N. Heurieux, W. R. Browne and B. L. Feringa, *Chem.–Eur. J.*, 2008, **14**, 3146–3153.
- 82 Y. Wang, R. M. Hernandez, D. J. Bartlett, J. M. Bingham, T. R. Kline, A. Sen and T. E. Mallouk, *Langmuir*, 2006, **22**, 10451–10456.
- 83 J. G. Gibbs and Y. P. Zhao, *Appl. Phys. Lett.*, 2009, **94**, 163104.
- 84 Z. Fattah, G. Loget, V. Lapeyre, P. Garrigue, C. Warakulwit, J. Limtrakul, L. Bouffier and A. Kuhn, *Electrochim. Acta*, 2011, **56**, 10562–10566.
- 85 K. M. Manesh, M. Cardona, R. Yuan, M. Clark, D. Kagan, S. Balasubramanian and J. Wang, *ACS Nano*, 2010, **4**, 1799–1804.
- 86 J. Burdick, R. Laocharoensuk, P. M. Wheat, J. D. Posner and J. Wang, *J. Am. Chem. Soc.*, 2008, **130**, 8164–8165.
- 87 P. Calvo-Marzal, K. M. Manesh, D. Kagan, S. Balasubramanian, M. Cardona, G.-U. Flechsig, J. Posner and J. Wang, *Chem. Commun.*, 2009, 4509–4511.
- 88 W. Gao, K. M. Manesh, J. Hua, S. Sattayasamitsathit and J. Wang, *Small*, 2011, **7**, 2047–2051.
- 89 Y. Wang, S.-T. Fei, Y.-M. Byun, P. E. Lammert, V. H. Crespi, A. Sen and T. E. Mallouk, *J. Am. Chem. Soc.*, 2009, **131**, 9926–9927.
- 90 G. Miño, T. Mallouk, T. Darnige, M. Hoyos, J. Dauchet, J. Dunstan, R. Soto, Y. Wang, A. Rousset and E. Clement, *Phys. Rev. Lett.*, 2011, **106**, 048102.
- 91 S. Sundararajan, P. E. Lammert, A. W. Zudans, V. H. Crespi and A. Sen, *Nano Lett.*, 2008, **8**, 1271–1276.
- 92 Y. Hong, N. Blackman, N. Kopp, A. Sen and D. Velegol, *Phys. Rev. Lett.*, 2007, **99**, 178103.
- 93 N. S. Zacharia, Z. S. Sadeq and G. A. Ozin, *Chem. Commun.*, 2009, 5856–5858.
- 94 T. Mirkovic, M. L. Foo, A. C. Arsenault, S. Fournier-Bidoz, N. S. Zacharia and G. A. Ozin, *Nat. Nanotechnol.*, 2007, **2**, 565–569.
- 95 J. Wang, *ACS Nano*, 2009, **3**, 4–9.
- 96 T. Mirkovic, N. S. Zacharia, G. D. Scholes and G. A. Ozin, *ACS Nano*, 2010, **4**, 1782–1789.
- 97 M. Pumera, *Nanoscale*, 2010, **2**, 1643–1649.
- 98 T. E. Mallouk and A. Sen, *Sci. Am.*, 2009, **300**, 74–79.
- 99 S. J. Ebbens and J. R. Howse, *Soft Matter*, 2010, **6**, 726–738.
- 100 J. Wang and K. M. Manesh, *Small*, 2010, **6**, 338–345.
- 101 T. Isojima, M. Lattuada, J. B. Vander Sande and T. A. Hatton, *ACS Nano*, 2008, **2**, 1799–1806.
- 102 M. Himmelhaus and H. Takei, *Sens. Actuators, B*, 2000, **63**, 24–30.
- 103 S. M. Anthony, L. Hong, M. Kim and S. Granick, *Langmuir*, 2006, **22**, 9812–9815.
- 104 J. N. Anker and R. Kopelman, *Appl. Phys. Lett.*, 2003, **82**, 1102–1104.
- 105 J. Anker, *J. Appl. Phys.*, 2003, **93**, 6698.
- 106 J. N. Anker, C. J. Behrend, H. Huang and R. Kopelman, *J. Magn. Magn. Mater.*, 2005, **293**, 655–662.
- 107 C. J. Behrend, J. N. Anker, B. H. McNaughton and R. Kopelman, *J. Magn. Magn. Mater.*, 2005, **293**, 663–670.
- 108 B. H. McNaughton, R. R. Agayan, J. X. Wang and R. Kopelman, *Sens. Actuators, B*, 2007, **121**, 330–340.
- 109 J. Choi, Y. Zhao, D. Zhang, S. Chien and Y. H. Lo, *Nano Lett.*, 2003, **3**, 995–1000.
- 110 C. Behrend, *Appl. Phys. Lett.*, 2004, **84**, 154–156.
- 111 C. J. Behrend, J. N. Anker, B. H. McNaughton, M. Brasuel, M. A. Philbert and R. Kopelman, *J. Phys. Chem. B*, 2004, **108**, 10408–10414.
- 112 H. Wang and N. J. Halas, *Nano Lett.*, 2006, **6**, 2945–2948.
- 113 H. Y. Koo, D. K. Yi, S. J. Yoo and D. Y. Kim, *Adv. Mater.*, 2004, **16**, 274–277.
- 114 S. Pradhan, D. Ghosh and S. Chen, *ACS Appl. Mater. Interfaces*, 2009, **1**, 2060–2065.
- 115 X. Fu, J. Liu, H. Yang, J. Sun, X. Li, X. Zhang and Y. Jia, *Mater. Chem. Phys.*, 2011, **130**, 334–339.
- 116 S.-H. Hu and X. Gao, *J. Am. Chem. Soc.*, 2010, **132**, 7234–7237.
- 117 L. Petit, J.-P. Manaud, C. Mingotaud, S. Ravaine and E. Duguet, *Mater. Lett.*, 2001, **51**, 478–484.
- 118 S. Pradhan, L. Brown, J. Konopelski and S. Chen, *J. Nanopart. Res.*, 2009, **11**, 1895–1903.
- 119 X. Y. Ling, I. Y. Phang, C. Acikgoz, M. D. Yilmaz, M. A. Hempenius, G. J. Vancso and J. Huskens, *Angew. Chem., Int. Ed.*, 2009, **48**, 7677–7682.
- 120 J. C. Love, B. D. Gates, D. B. Wolfe, K. E. Paul and G. M. Whitesides, *Nano Lett.*, 2002, **2**, 891.
- 121 O. Cayre, V. N. Paunov and O. D. Velev, *J. Mater. Chem.*, 2003, **13**, 2445–2450.
- 122 S. Yang, J. Xu, Z. Wang, H. Zeng and Y. Lei, *J. Mater. Chem.*, 2011, **21**, 11930–11935.
- 123 A. S. Dimitrov and K. Nagayama, *Langmuir*, 1996, **12**, 1303–1311.
- 124 J.-Q. Cui and I. Kretschmar, *Langmuir*, 2006, **22**, 8281–8284.

- 125 K. Fujimoto, K. Nakahama, M. Shidara and H. Kawaguchi, *Langmuir*, 1999, **15**, 4630–4635.
- 126 B. J. Park and E. M. Furst, *Langmuir*, 2010, **26**, 10406–10410.
- 127 K. D. Anderson, M. Luo, R. Jakubiak, R. R. Naik, T. J. Bunning and V. V. Tsukruk, *Chem. Mater.*, 2010, **22**, 3259–3264.
- 128 J. Gong, X. Zu, Y. Li, W. Mu and Y. Deng, *J. Mater. Chem.*, 2011, **21**, 2067–2069.
- 129 B. Wang, B. Li, B. Zhao and C. Y. Li, *J. Am. Chem. Soc.*, 2008, **130**, 11594.
- 130 M. D. McConnell, M. J. Kraeutler, S. Yang and R. J. Composto, *Nano Lett.*, 2010, **10**, 603–609.
- 131 Z. Li, D. Lee, M. F. Rubner and R. E. Cohen, *Macromolecules*, 2005, **38**, 7876–7879.
- 132 Y. Lu, H. Xiong, X. Jiang, Y. Xia, M. Prentiss and G. M. Whitesides, *J. Am. Chem. Soc.*, 2003, **125**, 12724–12725.
- 133 R. T. Chen, B. W. Muir, G. K. Such, A. Postma, K. M. McLean and F. Caruso, *Chem. Commun.*, 2010, **46**, 5121–5123.
- 134 K. Nakahama, H. Kawaguchi and K. Fujimoto, *Langmuir*, 2000, **16**, 7882–7886.
- 135 C. Bae, J. Moon, H. Shin, J. Kim and M. M. Sung, *J. Am. Chem. Soc.*, 2007, **129**, 14232–14239.
- 136 Y. Yin, Y. Lu, B. Gates and Y. Xia, *J. Am. Chem. Soc.*, 2001, **123**, 8718–8729.
- 137 Y. Yin, Y. Lu and Y. Xia, *J. Am. Chem. Soc.*, 2001, **123**, 771–772.
- 138 T. R. Kline, M. Tian, J. Wang, A. Sen, M. W. Chan and T. E. Mallouk, *Inorg. Chem.*, 2006, **45**, 7555–7565.
- 139 S. b. Fournier-Bidoz, A. C. Arsenault, I. Manners and G. A. Ozin, *Chem. Commun.*, 2005, 441–443.
- 140 O. D. Velev, A. M. Lenhoff and E. W. Kaler, *Science*, 2000, **287**, 2240–2243.
- 141 J. R. Millman, K. H. Bhatt, B. G. Prevo and O. D. Velev, *Nat. Mater.*, 2005, **4**, 98–102.
- 142 M. Fialkowski, A. Bitner and B. A. Grzybowski, *Nat. Mater.*, 2005, **4**, 93–97.
- 143 O. D. Velev, B. G. Prevo and K. H. Bhatt, *Nature*, 2003, **426**, 515–516.
- 144 D. Dendukuri and P. S. Doyle, *Adv. Mater.*, 2009, **21**, 1–16.
- 145 A. B. Subramaniam, M. Abkarian and H. A. Stone, *Nat. Mater.*, 2005, **4**, 553–556.
- 146 R. F. Shepherd, J. C. Conrad, S. K. Rhodes, D. R. Link, M. Marquez, D. A. Weitz and J. A. Lewis, *Langmuir*, 2006, **22**, 8618–8622.
- 147 Z. Nie, W. Li, M. Seo, S. Xu and E. Kumacheva, *J. Am. Chem. Soc.*, 2006, **128**, 9408–9412.
- 148 T. Nisisako and T. Torii, *Lab Chip*, 2008, **8**, 287–293.
- 149 K.-H. Roh, D. C. Martin and J. Lahann, *Nat. Mater.*, 2005, **4**, 759–763.
- 150 S. Bhaskar, K. M. Pollock, M. Yoshida and J. Lahann, *Small*, 2010, **6**, 404–411.
- 151 Y. Srivastava, *Biomicrofluidics*, 2009, **3**, 012801.
- 152 N. K. Sheridan, US patent 4126854, 1978.
- 153 N. Sheridan, in *Flexible Flat Panel Displays*, John Wiley & Sons, Ltd, 2005, pp. 393–407.
- 154 C.-C. Ho, W.-S. Chen, T.-Y. Shie, J.-N. Lin and C. Kuo, *Langmuir*, 2008, **24**, 5663–5666.
- 155 H. Gu, Z. Yang, J. Gao, C. K. Chang and B. Xu, *J. Am. Chem. Soc.*, 2005, **127**, 34–35.
- 156 D. Li, Y. He and S. Wang, *J. Phys. Chem. C*, 2009, **113**, 12927–12929.
- 157 D. Suzuki, S. Tsuji and H. Kawaguchi, *J. Am. Chem. Soc.*, 2007, **129**, 8088–8089.
- 158 B. Liu, W. Wei, X. Qu and Z. Yang, *Angew. Chem., Int. Ed.*, 2008, **47**, 3973–3975.
- 159 J. Zhang, J. Jin and H. Zhao, *Langmuir*, 2009, **25**, 6431–6437.
- 160 Y. He and K. Li, *J. Colloid Interface Sci.*, 2007, **306**, 296–299.
- 161 J. Zhang, X. Wang, D. Wu, L. Liu and H. Zhao, *Chem. Mater.*, 2009, **21**, 4012–4018.
- 162 L. Hong, S. Jiang and S. Granick, *Langmuir*, 2006, **22**, 9495.
- 163 S. Jiang, M. J. Schultz, Q. Chen, J. S. Moore and S. Granick, *Langmuir*, 2008, **24**, 10073–10077.
- 164 S. Jiang and S. Granick, *Langmuir*, 2008, **24**, 2438–2445.
- 165 S. Berger, A. Synytska, L. Ionov, K.-J. Eichhorn and M. Stamm, *Macromolecules*, 2008, **41**, 9669–9676.
- 166 N. P. Pardhy and B. M. Budhlall, *Langmuir*, 2010, **26**, 13130–13141.
- 167 A. Perro, F. Meunier, V. Schmitt and S. Ravaine, *Colloids Surf., A*, 2009, **332**, 57–62.
- 168 B. Liu, C. Zhang, J. Liu, X. Qu and Z. Yang, *Chem. Commun.*, 2009, **26**, 3871–3873.
- 169 S.-H. Kim, G.-R. Yi, K. H. Kim and S.-M. Yang, *Langmuir*, 2008, **24**, 2365–2371.
- 170 C. Poncet-Legrand, L. Petit, S. Reculosa, C. Mingotaud, E. Duguet and S. Ravaine, *Prog. Colloid Polym. Sci.*, 2004, **123**, 240–244.
- 171 M. Lattuada and T. A. Hatton, *J. Am. Chem. Soc.*, 2007, **129**, 12878–12889.
- 172 M. Bradley and J. Rowe, *Soft Matter*, 2009, **5**, 3114–3139.
- 173 L. Nie, S. Liu, W. Shen, D. Chen and M. Jiang, *Angew. Chem., Int. Ed.*, 2007, **46**, 6321–6324.
- 174 J. Mao, X. Qi, X. Cao, J. Lu, Q. Xu and H. Gu, *Chem. Commun.*, 2011, **47**, 4228–4230.
- 175 S. Zhang, Z. Li, S. Samarajeewa, G. Sun, C. Yang and K. L. Wooley, *J. Am. Chem. Soc.*, 2011, **133**, 11046–11049.
- 176 E. B. Mock, H. De Bruyn, B. S. Hawkett, R. G. Gilbert and C. F. Zukoski, *Langmuir*, 2006, **22**, 4037–4043.
- 177 J.-W. Kim, R. J. Larsen and D. A. Weitz, *J. Am. Chem. Soc.*, 2006, **128**, 14374–14377.
- 178 E. B. Mock and C. F. Zukoski, *Langmuir*, 2010, **26**, 13747–13750.
- 179 A. Pfau, R. Sander and S. Kirsch, *Langmuir*, 2002, **18**, 2880–2887.
- 180 C. Tang, C. Zhang, J. Liu, X. Qu, J. Li and Z. Yang, *Macromolecules*, 2010, **43**, 5114–5120.
- 181 J. W. Kim, R. J. Larsen and D. A. Weitz, *Adv. Mater.*, 2007, **19**, 2005–2009.
- 182 D. Nagao, M. Hashimoto, K. Hayasaka and M. Konno, *Macromol. Rapid Commun.*, 2008, **29**, 1484–1488.
- 183 D. Nagao, C. M. van Kats, K. Hayasaka, M. Sugimoto, M. Konno, A. Imhof and A. van Blaaderen, *Langmuir*, 2010, **26**, 5208–5212.
- 184 S. Reculosa, C. l. Poncet-Legrand, A. Perro, E. Duguet, E. Bourgeat-Lami, C. Mingotaud and S. Ravaine, *Chem. Mater.*, 2005, **17**, 3338–3344.
- 185 A. Perro, S. Reculosa, F. Pereira, M.-H. Delville, C. Mingotaud, E. Duguet, E. Bourgeat-Lami and S. Ravaine, *Chem. Commun.*, 2005, 5542–5543.
- 186 J. Ge, Y. Hu, T. Zhang and Y. Yin, *J. Am. Chem. Soc.*, 2007, **129**, 8974–8975.
- 187 T. Fujibayashi, T. Tanaka, H. Minami and M. Okubo, *Colloid Polym. Sci.*, 2010, **288**, 879–886.
- 188 D. Nagao, K. Goto, H. Ishii and M. Konno, *Langmuir*, 2011, **27**, 13302–13307.
- 189 M. M. Rahman, F. Montagne, H. Fessi and A. Elaissari, *Soft Matter*, 2011, **7**, 1483–1490.
- 190 W. Lu, M. Chen and L. Wu, *J. Colloid Interface Sci.*, 2008, **328**, 98–102.
- 191 B. M. Teo, S. K. Suh, T. A. Hatton, M. Ashokkumar and F. Grieser, *Langmuir*, 2011, **27**, 30–33.
- 192 Y. Wang, C. Zhang, C. Tang, J. Li, K. Shen, J. Liu, X. Qu, J. Li, Q. Wang and Z. Yang, *Macromolecules*, 2011, **44**, 3787–3794.
- 193 A. Misra and M. W. Urban, *Macromol. Rapid Commun.*, 2010, **31**, 119–127.
- 194 T. Kietzke, D. Neher, M. Kumke, O. Ghazy, U. Ziener and K. Landfester, *Small*, 2007, **3**, 1041–1048.
- 195 N. Saito, Y. Kagari and M. Okubo, *Langmuir*, 2006, **22**, 9397–9402.
- 196 X. Ge, M. Wang, X. Ji, X. Ge and H. Liu, *Colloid Polym. Sci.*, 2009, **287**, 819–827.
- 197 T. Tanaka, R. Nakatsuru, Y. Kagari, N. Saito and M. Okubo, *Langmuir*, 2008, **24**, 12267–12271.
- 198 T. Tanaka, M. Okayama, Y. Kitayama, Y. Kagawa and M. Okubo, *Langmuir*, 2010, **26**, 7843–7847.
- 199 T. Isojima, S. K. Suh, J. B. Vander Sande and T. A. Hatton, *Langmuir*, 2009, **25**, 8292–8298.
- 200 H. Yabu, T. Higuchi, K. Ijiri and M. Shimomura, *Chaos*, 2005, **15**, 047505.
- 201 T. Higuchi, A. Tajima, K. Motoyoshi, H. Yabu and M. Shimomura, *Angew. Chem., Int. Ed.*, 2008, **47**, 8044–8046.
- 202 H. K. Yu, Z. Mao and D. Wang, *J. Am. Chem. Soc.*, 2009, **131**, 6366–6367.
- 203 C. Zhang, B. Liu, C. Tang, J. Liu, X. Qu, J. Li and Z. Yang, *Chem. Commun.*, 2010, **46**, 4610–4612.
- 204 A. Ohnuma, E. C. Cho, P. H. C. Camargo, L. Au, B. Ohtani and Y. Xia, *J. Am. Chem. Soc.*, 2009, **131**, 1352–1353.

- 205 S. Xing, Y. Feng, Y. Y. Tay, T. Chen, J. Xu, M. Pan, J. He, H. H. Hng, Q. Yan and H. Chen, *J. Am. Chem. Soc.*, 2010, **132**, 9537–9539.
- 206 M. Feyen, C. Weidenthaler, F. Schüth and A.-H. Lu, *J. Am. Chem. Soc.*, 2010, **132**, 6791–6799.
- 207 Z. Bo, J. P. Rabe and A. D. Schlüter, *Angew. Chem., Int. Ed.*, 1999, **38**, 2370–2372.
- 208 A. D. Schlüter and J. P. Rabe, *Angew. Chem., Int. Ed.*, 2000, **39**, 864–883.
- 209 K. Ishizu, J. Satoh and K. Tsubaki, *J. Mater. Sci. Lett.*, 2001, **20**, 2253–2256.
- 210 D. Lanson, M. Schappacher, R. Borsali and A. Deffieux, *Macromolecules*, 2007, **40**, 9503–9509.
- 211 D. Lanson, M. Schappacher, R. Borsali and A. Deffieux, *Macromolecules*, 2007, **40**, 5559–5565.
- 212 L. Cheng, G. Hou, J. Miao, D. Chen, M. Jiang and L. Zhu, *Macromolecules*, 2008, **41**, 8159–8166.
- 213 T. Chen, G. Chen, S. Xing, T. Wu and H. Chen, *Chem. Mater.*, 2010, **22**, 3826–3828.
- 214 I. K. Voets, A. de Keizer, P. de Waard, P. M. Frederik, P. H. H. Bomans, H. Schmalz, A. Walther, S. M. King, F. A. M. Leermakers and M. A. Cohen Stuart, *Angew. Chem., Int. Ed.*, 2006, **45**, 6673–6676.
- 215 I. K. Voets, R. Fokkink, T. Hellweg, S. M. King, P. d. Waard, A. d. Keizer and M. A. Cohen Stuart, *Soft Matter*, 2009, **5**, 999–1005.
- 216 F. Wurm, H. M. König, S. Hilf and A. F. M. Kilbinger, *J. Am. Chem. Soc.*, 2008, **130**, 5876–5877.
- 217 J. Du and S. P. Armes, *Soft Matter*, 2010, **6**, 4851–4857.
- 218 B. Fang, A. Walther, A. Wolf, Y. Xu, J. Yuan and A. H. E. Müller, *Angew. Chem., Int. Ed.*, 2009, **48**, 2877–2880.
- 219 E. Hoppenbrouwers, Z. Li and G. Liu, *Macromolecules*, 2003, **36**, 876–881.
- 220 L. Cheng, G. Zhang, L. Zhu, D. Chen and M. Jiang, *Angew. Chem., Int. Ed.*, 2008, **47**, 10174–10171.
- 221 X. Li, H. Yang, L. Xu, X. Fu, H. Guo and X. Zhang, *Macromol. Chem. Phys.*, 2010, **211**, 297–302.
- 222 J. Dupont and G. Liu, *Soft Matter*, 2010, **6**, 3654–3661.
- 223 R. Saito, A. Fujita, A. Ichimura and K. Ishizu, *J. Polym. Sci., Part A: Polym. Chem.*, 2000, **38**, 2091–2097.
- 224 R. Erhardt, A. Böker, H. Zettl, H. Kaya, W. Pyckhout-Hintzen, G. Krausch, V. Abetz and A. H. E. Müller, *Macromolecules*, 2001, **34**, 1069–1075.
- 225 R. Erhardt, M. Zhang, A. Böker, H. Zettl, C. Abetz, P. Frederik, G. Krausch, V. Abetz and A. H. E. Müller, *J. Am. Chem. Soc.*, 2003, **125**, 3260–3267.
- 226 Y. Liu, V. Abetz and A. H. E. Müller, *Macromolecules*, 2003, **36**, 7894–7898.
- 227 A. Walther, X. André, M. Drechsler, V. Abetz and A. H. E. Müller, *J. Am. Chem. Soc.*, 2007, **129**, 6187–6198.
- 228 R. N. Klupp Taylor, H. Bao, C. Tian, S. Vasylyev and W. Peukert, *Langmuir*, 2010, **26**, 13564–13571.
- 229 H. Bao, W. Peukert and R. K. Taylor, *Adv. Mater.*, 2011, **23**, 2644–2649.
- 230 M. Giersig, P. Mulvaney, T. Ung and L. M. Liz-Marzán, *Adv. Mater.*, 1997, **9**, 570–575.
- 231 H. Gu, R. Zheng, X. Zhang and B. Xu, *J. Am. Chem. Soc.*, 2004, **126**, 5664–5665.
- 232 H. K. Yu, Z. Mao and D. Wang, *J. Am. Chem. Soc.*, 2009, **131**, 6366–6367.
- 233 B. Grüning, U. Holtschmidt, G. Koerner and G. Rossmy, US patent 4715986, 1987.
- 234 F. Liang, J. Liu, C. Zhang, X. Qu, J. Li and Z. Yang, *Chem. Commun.*, 2011, **47**, 1231–1233.
- 235 M. R. Rasch, E. Rossinyol, J. L. Hueso, B. W. Goodfellow, J. Arbiol and B. A. Korgel, *Nano Lett.*, 2010, **10**, 3733–3739.
- 236 D. A. Christian, A. Tian, W. G. Ellenbroek, I. Levental, K. Rajagopal, P. A. Janmey, A. J. Liu, T. Baumgart and D. E. Discher, *Nat. Mater.*, 2009, **8**, 843–849.
- 237 T. Chen, M. Yang, X. Wang, L. H. Tan and H. Chen, *J. Am. Chem. Soc.*, 2008, **130**, 11858–11859.
- 238 L. H. Tan, S. Xing, T. Chen, G. Chen, X. Huang, H. Zhang and H. Chen, *ACS Nano*, 2009, **3**, 3469–3474.
- 239 S. E. Habas, P. Yang and T. Mokari, *J. Am. Chem. Soc.*, 2008, **130**, 3294–3295.
- 240 S. Kudera, L. Carbone, M. F. Casula, R. Cingolani, A. Falqui, E. Snoeck, W. J. Parak and L. Manna, *Nano Lett.*, 2005, **5**, 445–449.
- 241 S. Deka, A. Falqui, G. Bertoni, C. Sangregorio, G. Ponetti, G. Morello, M. D. Giorgi, C. Giannini, R. Cingolani, L. Manna and P. D. Cozzoli, *J. Am. Chem. Soc.*, 2009, **131**, 12817–12828.
- 242 S. Chakraborty, J. A. Yang, Y. M. Tan, N. Mishra and Y. Chan, *Angew. Chem., Int. Ed.*, 2010, **49**, 2888–2892.
- 243 A. Figuerola, I. R. Franchini, A. Fiore, R. Mastria, A. Falqui, G. Bertoni, S. Bals, G. Van Tendeloo, S. Kudera, R. Cingolani and L. Manna, *Adv. Mater.*, 2009, **21**, 550–554.
- 244 R. Buonsanti, V. Grillo, E. Carlino, C. Giannini, M. L. Curri, C. Innocenti, C. Sangregorio, K. Achterhold, F. G. n. Parak, A. Agostiano and P. D. Cozzoli, *J. Am. Chem. Soc.*, 2006, **128**, 16953–16970.
- 245 M. Casavola, V. Grillo, E. Carlino, C. Giannini, F. Gozzo, E. Fernandez Pinel, M. A. Garcia, L. Manna, R. Cingolani and P. D. Cozzoli, *Nano Lett.*, 2007, **7**, 1386–1395.
- 246 C. Cheng, K. F. Yu, Y. Cai, K. K. Fung and N. Wang, *J. Phys. Chem. C*, 2007, **111**, 16712–16716.
- 247 T. P. Vinod, M. Yang, J. Kim and N. A. Kotov, *Langmuir*, 2009, **25**, 13545–13550.
- 248 J. Mao, X. Cao, J. Zhen, H. Shao, H. Gu, J. Lu and J. Y. Ying, *J. Mater. Chem.*, 2011, **21**, 11478–11481.
- 249 F. Wetz, K. Soulantica, A. Falqui, M. Respaud, E. Snoeck and B. Chaudret, *Angew. Chem., Int. Ed.*, 2007, **46**, 7079–7081.
- 250 T. Mokari, C. G. Sztrum, A. Salant, E. Rabani and U. Banin, *Nat. Mater.*, 2005, **4**, 855–863.
- 251 T. Mokari, E. Rothenberg, I. Popov, R. Costi and U. Banin, *Science*, 2004, **304**, 1787–1790.
- 252 L. Carbone, S. Kudera, C. Giannini, G. Ciccarella, R. Cingolani, P. D. Cozzoli and L. Manna, *J. Mater. Chem.*, 2006, **16**, 3952–3956.
- 253 L. Zhang, Y.-H. Dou and H.-C. Gu, *J. Colloid Interface Sci.*, 2006, **297**, 660–664.
- 254 Z. W. Seh, S. Liu, S.-Y. Zhang, M. S. Bharathi, H. Ramanarayan, M. Low, K. W. Shah, Y.-W. Zhang and M.-Y. Han, *Angew. Chem., Int. Ed.*, 2011, 10140–10143.
- 255 K.-W. Kwon and M. Shim, *J. Am. Chem. Soc.*, 2005, **127**, 10269–10275.
- 256 K.-W. Kwon, B. H. Lee and M. Shim, *Chem. Mater.*, 2006, **18**, 6357–6363.
- 257 M. Saruyama, Y.-G. So, K. Kimoto, S. Taguchi, Y. Kanemitsu and T. Teranishi, *J. Am. Chem. Soc.*, 2011, **133**, 17598–17601.
- 258 T. Teranishi, Y. Inoue, M. Nakaya, Y. Oumi and T. Sano, *J. Am. Chem. Soc.*, 2004, **126**, 9914–9915.
- 259 M. Saruyama, M. Kanehara and T. Teranishi, *Chem. Commun.*, 2009, 2724–2726.
- 260 S.-H. Choi, E.-G. Kim and T. Hyeon, *J. Am. Chem. Soc.*, 2006, **128**, 2520–2521.
- 261 H. Yu, M. Chen, P. M. Rice, S. X. Wang, R. L. White and S. Sun, *Nano Lett.*, 2005, **5**, 379–382.
- 262 W. Shi, Y. Sahoo, H. Zeng, Y. Ding, M. T. Swihart and P. N. Prasad, *Adv. Mater.*, 2006, **18**, 1889–1894.
- 263 T. Pellegrino, A. Fiore, E. Carlino, C. Giannini, P. D. Cozzoli, G. Ciccarella, M. Respaud, L. Palmirotta, R. Cingolani and L. Manna, *J. Am. Chem. Soc.*, 2006, **128**, 6690–6698.
- 264 X. Wang, X. Kong, Y. Yu and H. Zhang, *J. Phys. Chem. C*, 2007, **111**, 3836–3841.
- 265 G. S. Chaubey, V. Nandwana, N. Poudyal, C.-b. Rong and J. P. Liu, *Chem. Mater.*, 2008, **20**, 475–478.
- 266 X. Gao, L. Yu, R. MacCuspie and H. Matsui, *Adv. Mater.*, 2005, **17**, 426–429.
- 267 G. Zhu and Z. Xu, *J. Am. Chem. Soc.*, 2011, **133**, 148–157.
- 268 L. Zhang, F. Zhang, W.-F. Dong, J.-F. Song, Q.-S. Huo and H.-B. Sun, *Chem. Commun.*, 2011, **47**, 1225–1227.
- 269 N. Zhao and M. Gao, *Adv. Mater.*, 2009, **21**, 184–187.
- 270 J. G. Duque, J. A. Eukel, M. Pasquali and H. K. Schmidt, *J. Phys. Chem. C*, 2009, **113**, 18863–18869.
- 271 J. G. Duque, M. Pasquali and H. K. Schmidt, *J. Am. Chem. Soc.*, 2008, **130**, 15340–15347.
- 272 G. Loget and A. Kuhn, *Anal. Bioanal. Chem.*, 2011, **400**, 1691–1704.
- 273 H. Reiche, W. W. Dunn and A. J. Bard, *J. Phys. Chem.*, 1979, **83**, 2248–2251.
- 274 C. Pacholski, A. Kornowski and H. Weller, *Angew. Chem., Int. Ed.*, 2004, **43**, 4774–4777.

- 275 L. Carbone, A. Jakab, Y. Khalavka and C. Sönnichsen, *Nano Lett.*, 2009, **9**, 3710–3714.
- 276 G. Menagen, J. E. Macdonald, Y. Shemesh, I. Popov and U. Banin, *J. Am. Chem. Soc.*, 2009, **131**, 17406–17411.
- 277 F. Mavr , R. K. Anand, D. R. Laws, K.-F. Chow, B.-Y. Chang, J. A. Crooks and R. M. Crooks, *Anal. Chem.*, 2010, **82**, 8766–8774.
- 278 J.-C. Bradley and Z. Ma, *Angew. Chem., Int. Ed.*, 1999, **38**, 1663–1666.
- 279 J.-C. Bradley, S. Babu, A. Mittal, P. Ndungu, B. Carroll and B. Samuel, *J. Electrochem. Soc.*, 2001, **148**, C647–C651.
- 280 J.-C. Bradley, S. Babu and P. Ndungu, *Fullerenes, Nanotubes, Carbon Nanostruct.*, 2005, **13**, 227–237.
- 281 S. Babu, P. Ndungu, J.-C. Bradley, M. P. Rossi and Y. Gogotsi, *Microfluid. Nanofluid.*, 2005, **1**, 284–288.
- 282 C. Warakulwit, T. Nguyen, J. Majimel, M.-H. Delville, V. Lapeyre, P. Garrigue, V. Ravaine, J. Limtrakul and A. Kuhn, *Nano Lett.*, 2008, **8**, 500–504.
- 283 G. Loget, V. Lapeyre, P. Garrigue, C. Warakulwit, J. Limtrakul, M.-H. Delville and A. Kuhn, *Chem. Mater.*, 2011, **23**, 2595–2599.
- 284 G. Loget, J. Roche and A. Kuhn, *Adv. Mater.*, 2012, in press.
- 285 G. Loget, T.-C. Lee, R. W. Taylor, S. Mahajan, O. Nicoletti, S. T. Jones, R. J. Coulston, V. Lapeyre, P. Garrigue, P. A. Midgley, O. A. Scherman, J. J. Baumberg and A. Kuhn, *Small*, 2012, in press.